Elemental analysis of wood materials by external millibeam thick target PIXE

Kjell-Erik Saarela

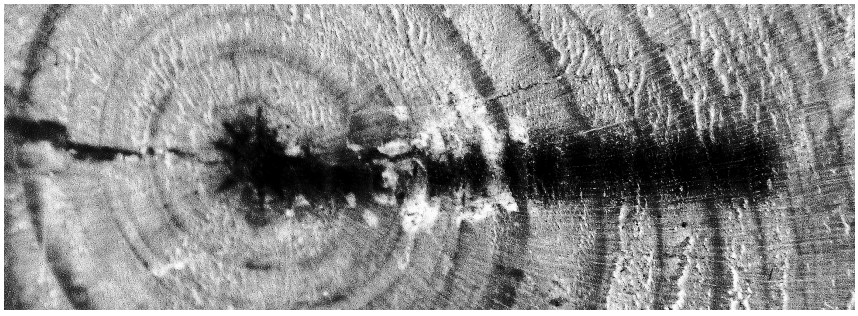

Process Chemistry Centre
Laboratory of Analytical Chemistry
Faculty of Mathematics and Natural Sciences
and
Accelerator Laboratory
Åbo Akademi University
Åbo, Finland
2009

ISBN 978-952-12-2347-1

UNIPRINT
Åbo 2009

Table of contents

PREFACE

The availability of a particle accelerator has made it possible to establish a Particle Induced X-ray Emission (PIXE) spectrometry activity at the Åbo Akademi University. An ambition in the development work has been towards an adaption that makes use of the most unique features of the PIXE method and serves as a complement to the many well established wet chemical methods available. What we have is a set-up for external (in air) thick target PIXE (TTPIXE), which can be used, e.g., for the direct analyses of solid biological materials, or the ashes of these materials, without preceding dissolution.

This thesis describes the instrumentation and methodology for the PIXE analyses of wood materials, and presents and discusses results obtained with the method. A chapter of general introduction of PIXE is followed by a chapter (2) dealing with the external thick target set-up and the methodology used in this thesis. In the last chapter (3) results from analyses of stem wood and bark are summarized and evaluated.

The above division also well describes my involvement and contributions to the PIXE activity. I came in contact with PIXE through my training/running companion, Mr. Jan-Olof Lill, at the beginning of the 1990s. At this time the thick target application of PIXE was introduced at the Accelerator Laboratory to replace the thin target application used up to then for analyses of clinical samples. Problems that had to be dealt with were related to, for example, sample preparation and quantification of the analyses. I found the possibility to analyse solid biological samples, with a method that combined multi-elemental character and high sensitivity for many of the elements, interesting and was glad to be able to take part in the development work. Dr. Lill has been the main architect of the PIXE set-up and thus a backbone of the activity. He has been the always available source of information for us non physicists, and data programming and calculation work has also been mostly his “table”. Thanks for your efforts Julle! Since the first visit to the basement of the Gadolinia building my physique is worse, while my knowledge in certain areas of physics has clearly improved.

I further want to thank the other, former or present, members of the PIXE group: I thank the director of the Accelerator Laboratory, Dr. Sven-Johan Heselius, for his supportive attitude, and for making the final linguistic improvements to most of our manuscripts. The many discussions during late nights at the Accelerator Laboratory with the gentlemen Julle, Hese, Leo Harju, Alf Lindroos, Johan Rajander, and others, are remembered with joy. The good cooperation with Johan and Mr. Stig-Göran Huldén also made the teaching of chemistry enjoyable. The closest cooperation in the environmental field has been with docent Leo Harju, not only because he always has had a reliable car available for different kinds of field trips. Thanks for good coaching during the years passed! Leo and Professor Ari Ivaska made good suggestions and linguistic improvements during the process of completing this thesis. Ari’s patience and support is greatly appreciated.

Mr. Stefan Johansson, Mr. Per-Olof Eriksson and Mr. Erkki Stenvall are thanked for their skilful maintenance and operation of the cyclotron.

I thank, among others, Aki Pihlman (archaeologist at the Provincial Museum of Turku), Eero Kuokkanen (health inspector, city of Harjavalta), Kaj Mattsson (director of the Turunmaa Fishermen's Association, Pargas), Marku Lehto (Merimasku), Kari Saari (environmental manager, UPM-Kymmene Pulp Centre, Jakobstad) and Fredrik Smedman (chemistry teacher, Nykarleby) for help with sampling of the pine, spruce and birch samples.

I thank Ilmari, Lisbeth, Jan and Tom for the happy times together, when wood was collected only because the kitchen and the tiled stove had to be kept warm.

The economical support from the Foundation for Research of Natural Resources in Finland, the Kone Foundation, the Research Institute of the Åbo Akademi Foundation, and the grant obtained through the steering group for the environmental profiling of the Åbo Akademi University (own translation from Swedish), that enabled the completion of this thesis, is gratefully acknowledged.

My final, and biggest, thanks go to Annica and our common, main projects Erica, Emma, Pontus and Elin.

Åbo, October 2009

Kjell-Erik Saarela

LIST OF INCLUDED PUBLICATIONS

This thesis is a summary of the following papers, referred to in the text by their corresponding Roman numerals.

I. L. Harju, J-O. Lill, K-E. Saarela, S-J. Heselius, F.J. Hernberg and A. Lindroos, Study of seasonal variations of trace-element concentrations within tree rings by thick-target PIXE analyses, Nucl. Instr. and Meth. B109/110 (1996): 536-541.

II. K-E Saarela, J-O Lill, F.J. Hernberg, L. Harju, A. Lindroos and S-J. Heselius, Preconcentration of trace elements in biological materials by dry ashing for TTPIXE analysis. A study of matrix effects, Nucl. Instr. and Meth., B103 (1995): 466-472.

III. L. Harju, J-O. Lill, K-E. Saarela, S-J. Heselius, F. J. Hernberg and A. Lindroos, Analysis of trace elements in trunk wood by thick target PIXE using dry ashing for preconcentration, Fresenius J. Anal. Chem. 358(1997): 523-528.

IV. K-E. Saarela, L. Harju, J-O. Lill, J. Rajander, A. Lindroos, S-J. Heselius and K. Saari, Thick-target PIXE analysis of trace elements in wood incoming to a pulp mill, Holzforschung 56 (2002): 380-387.

V. K-E. Saarela, L. Harju, J. Rajander, J-O. Lill, S-J. Heselius, A. Lindroos and K. Mattsson, Elemental analyses of pine bark and wood in an environmental study, Science of the Total Environment 343 (2005): 231-241.

VI. K-E. Saarela, L. Harju, J-O. Lill, S-J. Heselius, J. Rajander and A. Lindroos, Quantitative elemental analysis of dry-ashed bark and wood samples of birch, spruce and pine from south-western Finland using PIXE, Acta Academiae Aboensis, ser B, vol. 65, no. 4, Åbo Akademi University Press (2005), 27 pages (ISBN 951-765-269-0).

The author of this thesis has been the member of the research team focusing on the sampling, sample preparation and quantitative analyses of stem wood and bark from trees, and has been actively involved in the writing all papers I-VI. The author introduced the idea to prepare ashes of these materials for irradiation, as well as the idea to use the ratio between the concentration of an element in the ashes of stem bark to that in the ashes of the stem wood of a tree for the monitoring of atmospheric pollution, and was the main author of papers II, IV and V, as well as of the comprehensive paper VI.

Supporting publications, not included in this thesis

1. K-E Saarela, J-O. Lill, S-J. Heselius and V. Näntö, Elemental analysis of small tissue samples using Thick-Target PIXE, In: Proc. 6th Symp. Medical Application of Cyclotrons, Turku, June 1-4, 1992, Eds. L-M. Voipio-Pulkki and U. Wegelius, Ann. Univ.Turkuensis D88 (1992): A131.

2. J-O. Lill, K-E. Saarela, F.J. Hernberg, S-J Heselius and L. Harju, A novel method for charge integration in external beam TTPIXE. Application to analyses of biological materials, Nucl. Instr. and Meth. B83(1993): 387-393.

3. A. Lindroos, J-O. Lill, K-E Saarela, L. Harju and S-J Heselius, Determination of trace elemental profiles in coarse-grained schorl tourmaline minerals by external millibeam PIXE- A schorl tourmaline study, Bull. Geol. Soc. Finland, part 1, **67** (1995): 47-59.

4. L. Harju, J-O. Lill, K-E. Saarela, S-J. Heselius, F. Hernberg and A. Lindroos, Study of of seasonal variations of trace element concentrations within tree rings by Thick-target PIXE analyses, In: VII International Conference on Particle Induced X-ray Emission and its Analytical application, Padua, Italy, May 26-30, 1995, Program and Abstract Book, p. 73-74.

5. K-E. Saarela, J-O. Lill, L. Harju, A. Lindroos and S-J. Heselius, Evaluation of honey as a bioindicator material by Thick-Target PIXE, In: H. Högmander and A. Oikari (Eds.) Proc.Third Finnish Conference of Environmental Sciences, Jyväskylä, May 9-10, 1997, p. 261-264.

6. K-E. Saarela, J-O. Lill, L. Harju, A. Lindroos and S-J. Heselius, Multielement analyses of ashed honey samples by TTPIXE, Intern. J. Environ. Anal. Chem. 69(1998): 273-285.

7. J-O. Lill, L. Harju, K-E. Saarela, A. Lindroos and S-J. Heselius, Increased sensitivity in thick-target PIXE analyses using dry ashing for preconcentration, Anal. Chim. Acta. 378(1999): 273-278.

8. K-E Saarela, L. Harju, J-O. Lill, J. Rajander, A. Lindroos and S-J. Heselius, Thick-target PIXE analysis of chromium, copper and arsenic impregnated lumber, Nucl. Instr. and Meth. B150(1999): 234-239.

9. J. Rajander, L. Harju, J-O. Lill, K-E. Saarela, A. Lindroos and S-J. Heselius, Monitoring of chromium, copper and arsenic in contaminated soil using thick-target PIXE, Nucl. Instr. and Meth. B150(1999): 510-515.

10. K-E. Saarela, L. Harju, J-O. Lill, J. Rajander, A. Lindroos and S-J. Heselius, Thick-target PIGE-analysis of plant material preconcentrated by dry ashing, Talanta 51(2000): 717-725.

11. L. Harju, K-E. Saarela, J. Rajander, J-O. Lill, A. Lindroos and S-J Heselius, Environmental monitoring of trace elements in bark of Scots pine by thick-target PIXE, Nucl. Instr. and Meth. B 189(2002):303-307.

12. K-E Saarela, L. Harju, J-O. Lill, J. Rajander, A. Lindroos and S-J. Heselius, Elemental analyses of wood using dry ashing and PIXE In: 18th Nordic Conference on the measurement of elements and their compounds, Naantali, Finland 18-21.8 2002, Scientific Programme and Abstracts book, p. 41.

13. L. Harju, J. Rajander, K-E. Saarela, J-O. Lill, S-J. Heselius, A. Lindroos, Losses of elements during dry ashing of biological materials, Proc. 10th Int. Conf. on Particle Induced X-ray Emission and its Analytical Applications, Portorož, Slovenia, June 4-8, 2004, 945.1-3.

14. L. Harju, J. Rajander, K-E. Saarela, J-O. Lill, S-J- Heselies and A. Lindroos, Losses of elements during dry ashing of biological materials, Proc. 10th Int. Conf. on Particle Induced X-ray Emission and its analytical applications, Portorož, Slovenia, June 4-8, 2004 (Eds M. Budnar and M. Kavči), Electronic edition, Ljubljana (2004) p. 945.1-3.

1. INTRODUCTION

1.1. A general introduction to PIXE

PIXE is the acronym for Particle Induced X-ray Emission. PIXE spectrometry is based on the use of accelerated, charged particles. The fact that the analytical technique relies on the availability of a particle accelerator has limited a more widespread use of the ion beam technique. In practise the letter P in the acronym also could stand for proton because these are the particles mostly used.

In PIXE analyses the material analysed is bombarded with protons that cause electrons to be ejected from the inner shells of sample elements. X-rays are emitted when these vacancies are reoccupied. This radiation can be detected and used for qualitative and quantitative analysis of the sample material.

PIXE analysis requires the access to an energy dispersive detector to detect X-rays of different energies, emitted from the sample during particle irradiation. The signals from the detector are amplified, converted (A/D) and stored as counts of photons in the energy spectrum.

The counts within the peaks of an accumulated X-ray spectrum form the basis for quantification of the concentration of the elements. The number of characteristic photons detected is, however, proportional to the amount of protons the sample is irradiated with during the acquisition. An experimental set-up for PIXE analysis must therefore also include a method for measuring this charge (integrated beam current over acquisition time) if quantitative analysis are to be performed.

Strengths of the method are the multielement character and the possibility to analyse even very small amounts of sample material. Elemental distributions in solid materials can be studied down to a level restricted by the diameter of the particle beam used.

The advantage of PIXE compared to methods where electrons are used for excitation is related to the larger mass of the proton. The heavier proton induces more element specific X-ray emission relative to the unspecific, continuous background radiation produced (spectral background in the form of *bremsstrahlung*). The spectral background in PIXE is mainly from the retardation of electrons ejected from the atoms in the target sample (*secondary electron bremsstrahlung*). Detection limits in PIXE can be up to 100 times lower than for electron beam techniques because in the latter, electron bremsstrahlung is the primary, projectile, bremsstrahlung (Johansson et al. 1995).

1.2. X-ray production and the PIXE spectrum

1.2.1. Characteristic X-ray emission

In PIXE the sample is normally bombarded with accelerated protons with a kinetic energy of 2-3 MeV (Campbell and Cookson 1984, Maenhaut 1988). The protons create vacancies in the inner shells of target elements. Characteristic X-rays are emitted when these vacancies are filled with electrons from the outer shells, i.e. during de-excitation.

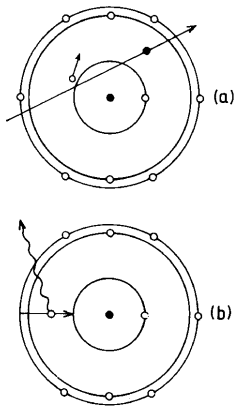

Figure 1. Accelerated protons inducing X-ray emission in a target sample: a) an incoming proton ejects an electron from the innermost shell of an atom b) the vacancy is filled with an electron from an outer shell and a characteristic X-ray (K_α) is emitted.

As excitations are through ejection of electrons from the inner shells, the characteristic radiation measured is basically independent of the chemical form of the element. If a vacancy is created in the innermost, K-shell (principle quantum number n = 1) and this vacancy is filled with an electron from the L-shell outside (n = 2) the corresponding (characteristic) radiation is named K_α, according to the Siegbahn notation (Johansson et al. 1995). If the transition is from an M- or N-shell the radiation is named K_β. The characteristic radiation from a vacancy in the L-shell being filled with an electron from the outer M-shell is named L_α.

The *cross section,* denoted by σ, is defined as the probability that a certain process will take place as the result of a collision between particles. The cross section expresses the effective surface a particle offers to this process (Maenhaut and Malmqvist 1992, Knoll 1979).

The *ionisation cross section* gives the probability that a vacancy will be created in a shell of the atom when it encounters a charged particle of a specific energy (E). The cross section is dependent on the energy of the incoming particle as well as on the atomic number of the target element (Z). The ionisation cross section is often denoted by $\sigma(E)$, or by $\boldsymbol{\sigma^I(E)}$ to be more clear (Maenhaut and Malmqvist 1992).

In PIXE analysis the excitation from the creation of a vacancy in the innermost shell (the K-shell) is mainly utilized. The K-shell ionisation cross section is, however, rather rapidly declining when going to elements of higher atomic numbers (Johansson and Campbell 1988). For heavy elements (like, for example, lead in biological materials), L-shell ionisations, and the corresponding L-lines emitted, are therefore often more useful.

The probability that an excited atom emits its excess energy in the form of a photon is expressed by the quantity *fluorescence yield,* denoted by **ω** (Johansson and Johansson 1976, Folkmann et al. 1974)**.** This probability is dependent on the atomic number of the element, and for K-lines it increases especially rapidly for atomic numbers Z > 10 (p. 11 in Johansson et al.1995). The probability of fluorescence is close to 1 for heavy elements. For light elements, on the other hand, the probability is only a few per cent (Johansson et al. 1995).

The probability of a certain characteristic X-ray being emitted when a proton encounters an element in the target material is named *X-ray production cross section*, and is denoted by $\boldsymbol{\sigma^{X}(E)}$ (Maenhaut and Malmqvist 1992). The X-ray production cross section for a K-line can, thus, be given as $\boldsymbol{\sigma^{I}(E)\cdot\omega\cdot b^{\alpha}}$**,** where the factor **b** represents the probability that the emitted radiation is, in this case, K_{α}. The *X-ray production cross section* thus varies with the energy of the protons.

Although lighter elements generally have higher ionisation cross sections the detection limits are higher for these elements. This is partially related to the fact that the fluorescent yield is lower for a lighter element (Johansson and Johansson 1976), and partially to the fact that the energy of the emitted photons decreases with the atomic number (Z) of the element. X-ray emission of lower energy is more strongly attenuated in the sample, in a detector window, or in any other absorber.

1.2.2. Bremsstrahlung and other components of the spectral background

When the speed or direction of an electrical charge in motion is altered, electromagnetic radiation is emitted (Knoll 1979). Retardation of charged particles in a material thus gives rise to a continuous, unspecific radiation (*bremsstrahlung*). Continuous radiation is emitted in PIXE when the incoming protons are retarded (primary bremsstrahlung). Most of the background radiation is, however, from ejected electrons in the target sample (secondary electron bremsstrahlung). A normal PIXE-spectrum consists basically of characteristic peaks residing on this continuous background.

The number of characteristic X-rays relative to the background, at the energy in question in the spectrum, is crucial for the detectability of the element emitting the characteristic radiation. This is also the reason why detection limits for electron probe techniques are generally much higher than for PIXE. The intensity of the bremsstrahlung is also higher, relative to the characteristic emission, if the matrix consists of heavier elements (Maenhaut and Malmqvist 1992), and this renders higher detection limits (Maenhaut 1988).

For energies < 3 keV in the PIXE spectrum the number of detected X-rays decreases sharply due to absorption in the sample itself, in the gas atmosphere between sample and detector, in the detector window or in any other external absorber (Szökefalvi-Nagy et al. 1999). A typical spectrum obtained in PIXE analysis performed at Åbo Akademi University is shown in Fig. 2.

The ionisation cross section is a fundamental parameter, considering the yields of characteristic X-rays, which value increases with increasing proton energies (Maenhaut and Malmqvist 1992). However, for higher proton energies bremsstrahlung is also extended to higher energies. Contributions from gamma-ray and neutron background (Teesdale et al. 1988, Räisänen 1987) also increase, and for proton energies > 3 MeV they can constitute the dominating component of the background in the higher energy region (> 10 keV) of the PIXE-spectrum (Johansson and Campbell 1988, Räisänen 1987).

If a majority of the characteristic X-rays registered are from a few dominating lighter elements, the low-energy X-rays can occupy most of the counting capacity of the detection system. In such a case it can be favourable to use an absorber for these softer X-rays, to increase the sensitivity for heavier elements (Johansson and Johansson 1976).

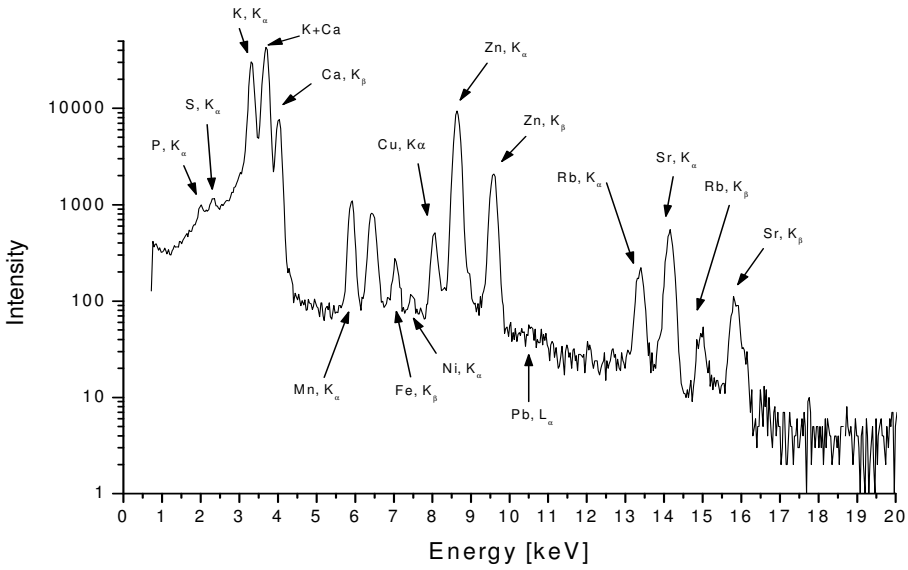

Figure 2. A PIXE-spectrum accumulated during irradiation of a thick sample of dry ashed wood material with 3 MeV protons (Wood Fuel, reference material NJV 94-5 from the Swedish University of Agricultural Sciences, Umeå, Sweden). A total charge of 1.7 μC was deposited during 10 minutes (beam current 2.8 nA, current density ca. 360 nA/cm^2). Characteristic emission lines are marked with the chemical symbol of the emitting element, together with the designation for the line.

1.3. Target samples in PIXE – thin or thick or something in between?

The PIXE technique can be divided into two main categories, based on the thickness of the irradiated sample target, as illustrated in Fig. 3. In thin target PIXE (Fig. 3a) the retardation of protons within the sample is assumed to be insignificant and the yield from an element is fully based on the ionisation cross section at the energy E_0, i.e. the energy of the proton at the target surface. A general upper limit of 1 mg sample material per cm^2 target surface, has been given for targets that can be considered as thin targets, (Johansson and Johansson 1976, Johansson and Campbell 1988). For a target consisting of 0.5 g of bovine liver per cm^2 of target surface, the matrix effects from retardation of protons and attenuation of induced X-rays have been found to be 3-5 % for elements K – Sn (Maenhaut and Malmqvist 1992), when 2.4 MeV protons are used.

In the second category, thick target PIXE (TTPIXE), the sample target is thick enough to fully stop the particles, and ionisation cross sections decrease as the energy goes from E_0 to 0 for the protons entering the sample material (Fig. 3b).

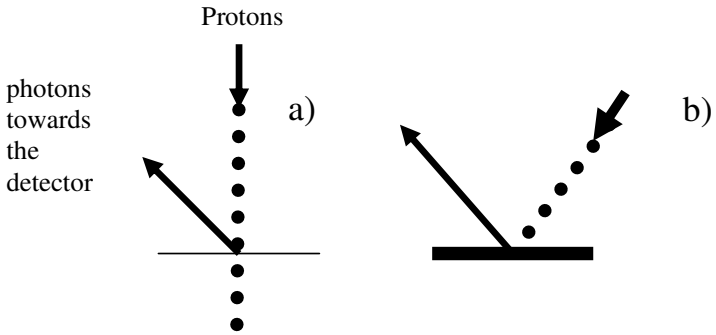

Figure 3. Illustration of: a) thin target PIXE, where protons pass through the sample material loosing only an insignificant part of their kinetic energy, and b) thick target PIXE, where the protons are fully stopped, i.e. lose all their kinetic energy.

1.3.1. Preparation of thin and thick target samples

Sample material rather seldom exists in a form that represents a thin target (Johansson et al. 1995). A field in which the thin target technique has been largely applied, is as standard method for analysing particulate material in air (aerosols), where thin layers of particles are collected on filters or foils (p. 237 in Johansson et al. 1995).

Liquid samples can be analysed as thin targets by depositing the solution on a thin foil and evaporating to dryness. Wet-chemical dissolution would thus be a way to prepare solid biological materials to thin targets for PIXE analyses. This pre-treatment procedure would, however, make PIXE compete with a large number of well established, and easily available, instrumental methods for analyses of liquid samples. Johansson and Campbell (1988) pointed

out that crystallisations give rise to locally thick segments in this kind of targets. It has also been concluded that target samples prepared by dissolution and pipetting cannot generally be considered thin, with negligible matrix effects (Pallon and Malmqvist 1981).

As small an amount as 15.4 mg of starch, equally distributed over an area of 1 cm^2, is enough to fully stop 3 MeV protons (see section 2.2.1). The amount of sample limiting preparation of thick samples thus mostly comes down to the question of what amount can be handled properly. Sample target preparation should end up with a flat surface of sample material facing the proton beam. Solid biological samples can, for example, be cut, or milled and pressed to pellets. The 3 MeV protons in a beam with a diameter of 1 mm pass through a maximum of about 0.2 mg of biological material (compare table 1 on page 16)). The majority of the X-rays reaching the detector are from an even much smaller amount of sample. If bulk analyses are to be performed, great attention should thus be paid to the homogeneity of the sample material from which a thick target is prepared

1.3.2. Yields of characteristic X-rays from absolutely thin targets

Irradiation with accelerated protons induces emission of characteristic X-rays from elements present in the target sample. The yield is the number of X-rays of a certain energy registered during irradiation of the sample (Johansson et al. 1995), which form the peak area at the characteristic photon energy in the X-ray spectrum. The yield is denoted by Y, and is dependent on a number of variables which for a K_α-line from an ideally thin sample can be summarised in equation (1):

$$Y(Z) = \frac{N_p m_Z}{A} \frac{\sigma_Z^I(E_0)\omega_Z b_Z^\alpha \varepsilon_Z^\alpha N_{Av}}{M_Z} \qquad (1)$$

The detected emission is from the element with atomic number Z, and

- N_p = the total number of protons on the target sample.
- A = the area of irradiated/penetrated surface.
- m_Z = the absolute mass of the element in the irradiated/penetrated volume of sample. For a uniformly thick surface this volume = A×thickness.
- $\sigma_Z^I(E_0)$ = the K-shell ionisation cross section of the element when the proton energy is E_0.
- ω_Z = the fluorescence yield for the element.
- b_Z^α = the proportion of K-radiation that is emitted as K_α.
- ε_Z^α = the total (absolute) detector efficiency for the emitted radiation, which is dependent on the measuring geometry, the intrinsic efficiency of the detector, absorbers (for example the detector window and other external absorbers and possible absorption of low energy X-rays in air between sample and detector).
- N_{Av} = Avogadro's number
- M_Z = the molar mass of the element

An element specific constant, k_Z, independent of the proton energy and including the total detector efficiency (i.e. it takes the set-up used into consideration), can be extracted from the above equation (1) as.

$$k_Z = \frac{\omega_Z b_Z^{\alpha} \varepsilon_Z^{\alpha} N_{Av}}{M_Z} \tag{2}$$

Since the mass per unit area can be written as: $\rho_Z d_X = \frac{m_Z}{A}$, where ρ_Z is the density (i.e. the mass of this element per volume of sample), and d_X the thickness of the target sample, the expression for the yield can be written as:

$$Y = k_Z N_p \sigma_Z^I(E_0) \rho_Z d_X \tag{3}$$

For a specific set-up (i.e. a certain detector, a constant geometry and beam cross section etc) and a specific proton energy the amount of characteristic x-rays from an element in an perfectly thin target sample is dependent only on the total charge deposited (N_p) and the amount of the element in the penetrated target layer.

1.3.3. Yields from targets that are not absolutely thin

The amount of characteristic X-ray induced, per deposited charge, is larger in a thicker target sample. For any target sample that is not perfectly thin, however, the type of matrix will affect the yield. When, for example, analyses of thick biological materials are performed, retardation of the protons, which leads to smaller ionisation cross sections, as well as attenuation of the X-rays from deeper within the target sample, will occur (Maenhaut 1987).

1.3.3.1. Retardation of protons

When a proton hits a sample it will lose kinetic energy mainly by coulomb interaction with bound electrons (Maenhaut and Malmqvist 1992). The stopping power represents the loss of energy per length unit in a material of a certain density, and is denoted by S:

$$\mathrm{S(E)} = \frac{1}{\rho} \cdot \frac{dE}{dx} \tag{4}$$

This quantity, specific for a certain material, depends on the energy of the protons. The loss of energy increases exponentially with decreasing proton energy. The unit of the energy loss is usually given as keV/(mg/cm^2)· Compilations of S(E)-values for different substances at different particle energies are available (Ziegler et al. 1985).

The range (x) for protons of the initial energy E_0 can be calculated according to equation (5)

$$x = \int_{Eo}^{0} \frac{dE}{\rho \cdot S(E)} \tag{5}$$

The stopping power for chemical compounds and mixtures is assumed to be a concentration weighed sum of contributions from the elements present (Maenhaut and Malmqvist 1992), as expressed by equation (6):

$$S_c = \sum_i w_i S_i(E) \tag{6}$$

where w_i denotes the mass fraction of the i:th element.

1.3.3.2. Attenuation of X-rays

The attenuation of specific photon energy, induced within a sample, depends on the composition and the density of the sample as well as the distance to the sample surface.

A monoenergetic photon beam of intensity I_0, passing through an absorbing material, will lose intensity according to equation (7):

$$I(x) = I_0 e^{-\mu x} \tag{7}$$

Here μ stands for the linear absorption coefficient, which could be explained as the probability for a photon to be lost from the photon beam after travelling a length unit in the material. The value of μ is higher for less energetic photons, which means that X-rays emitted from lighter elements are more strongly attenuated.

The intensity (I) of the X-ray emission out of the sample is proportional to the intensity (I_0) of the radiation at the point where it was induced, and decreases exponentially with the distance (x) travelled in the material. The ratio $I(x)/I_0$ is called transmission (T). The distance x to the surface, for induced X-ray emission of decreasing intensity down in deeper layers of the non-thin target, depends on the sample matrix and the measuring geometry of the experimental set-up. The transmission factor (Johansson et al. 1995) suffered by X-rays emitted towards the detector from a point within the sample, defined by the energy (E) of the protons, is given in equation 8.

$$T(E) = \exp\left\{ \left(-(\mu/\rho)_{Z,M} \cos\alpha / \sin\theta \int_{E_0}^{E} \frac{dE}{S_M(E)}\right) \right\} \tag{8}$$

Here $(\mu/\rho)_{Z,M}$ stands for the concentration weighted sum of attenuation coefficients of the matrix elements, experienced by emission from the analysed element (Z). The geometry is described by the angle between the particle beam and the normal to the sample surface (α), and the angle between the X-rays towards the detector and the sample surface (Θ)

1.3.3.3. Yields of characteristic X-rays from thick target samples

The yield for an element from a thick target is determined by the number of characteristic X-rays, induced down the stopping range of the protons, that reaches the surface of the sample in direction towards the detector. X-ray emission is induced with decreasing efficiency as protons are slowed down.

The expression for the yield from an absolute thin sample, given in equation (3), can be used as a basis for expressing the yield (dY) from an arbitrary, thin layer (dx) within a thick sample. Here the layer is assumed so thin that the energy of the protons (E) remains the same throughout

$$dY(Z) = k_Z N_p \sigma_Z^I(E) \rho_Z T(E) dx \tag{9}$$

The transmission factor T(E) in equation (9) gives the portion of X-rays induced reaching the sample surface in the direction towards the detector from this layer.

By substituting dx, the thickness of the layer, with an expression obtained from equation (4),

$$dx = \frac{1}{\rho} \cdot \frac{dE}{S(E)}$$

and after indexing with ”M” to indicate that the density and the stopping power is for the sample matrix, we obtain equation (10):

$$dY(Z) = k_Z N_p \sigma_Z^I(E) \rho_Z T(E) \frac{dE}{\rho_M S_M(E)} \tag{10}$$

The ratio ρ_Z / ρ_M in equation (10) can be replaced by the concentration of the element in question, C(Z). Integration of the obtained expression from the incident proton energy E_0 to 0 (protons completely stopped) gives equation (11):

$$Y(Z) = k_Z N_p C(Z) \int_{E_0}^{0} \frac{\sigma_Z^I(E) T(E)}{S_M(E)} dE \tag{11}$$

Here the yield, Y(Z), is the total number of the characteristic X-rays that are registered by the detection system. The yield is directly proportional to the concentration of the element and the number of particles incident on the target sample (N_p).

The relative contributions to the yield, from different depths in the thick sample, are dependent on the matrix effects and the geometry of the set-up. The matrix effects are considered by the integral in equation (11). A decreasing energy of the protons, means a lower ionisation cross section (σ^I), and thus also a proportionally lower X-ray production cross section for the analysed element. This, and the increased attenuation, of especially softer X-rays, will lead to lesser contributions from the deeper layers.

1.4. Internal or external PIXE – vacuum or gas atmosphere

PIXE analysis is often performed with the target sample placed in a vacuum chamber. An application where the chamber is connected to the accelerator vacuum is named internal PIXE. Vacuum is crucial in the so called micro-PIXE, where the proton beam is collimated down to 1 μm diameter and defocusing by scattering on gas molecules has to be avoided (Johansson et al. 1995).

The particle beam can also be extracted from the accelerator vacuum into a gas atmosphere through an extraction foil. Different from electron beam techniques a possible application of PIXE is to place the sample in air at normal pressure – i.e. to extract the proton beam into open air (Johansson and Campbell 1988). This application has been named external PIXE.

In a vacuum, the protons are not interacting with gas molecules. A contribution to spectral background from, e.g., air (Williams 1984, Doyle et al. 1991), as well as absorption of soft X-rays from the sample towards the detector, can thus be avoided (Williams 1984),

When organic materials are irradiated in a vacuum, two unwanted events occur: heating and charging of the sample (Clayton 1987). Historical pieces of art, paintings or manuscripts cannot, or should not, be analysed in a vacuum chamber (Wagner and Neelmeijer 1995). The cooling effect of gas molecules is lacking in vacuum. Low pressure over the sample also promotes volatilization of components during irradiation (Doyle et al. 1991). Biological samples therefore tend to lose volatile elements (Johansson and Campbell 1988).

When non-conducting samples, like biological materials, are irradiated in vacuum, charging occurs that has to be considered. The charging is especially pronounced when the sample is thick (Goclowski et al. 1983). Periodical discharging will occur, which adds *electron bremsstrahlung* to the spectral background (Teesdale et al. 1988, Goclowski et al. 1983). This extra bremsstrahlung from retardation of electrons accelerated in the discharge can reach over a large spectral interval and can become the main component of the background (Goclowski et al. 1983). Charging of a sample also causes variations in Coulomb force retarding the incoming protons. The energy of the protons reaching the sample surface will thus vary, which will affect the analytical result.

In external PIXE, ionized gas molecules in the beam path eliminate charge accumulation, thereby increasing the signal-to-back-ground ratio (Williams 1984, Goclowski et al. 1983).

Soft (low energy) X-rays are absorbed in air between the sample and the detector (Räisänen 1992, Williams 1984, Mando 1994), and the detector should therefore be placed close to the sample. This tight geometry is also a prerequisite for a large solid angle and high detection efficiency. Absorption of low energy X-rays is less in the case of a helium atmosphere. In this application a special chamber is, however, needed, limiting the flexibility for handling different type of samples (Williams 1984)

Katsanos and co-workers (Katsanos et al. 1976, Katsanos and Hadjiantonou 1978) analysed thick biological samples both in vacuum and in air. They concluded external PIXE to be better for elements with atomic numbers greater than 14 ($Z > 14$), at otherwise similar conditions. It was, however, stated that internal (vacuum) PIXE is the best method for lighter elements (Katsanos et al. 1976).

1.5. Measurement of the number of particles incident on the target sample

The area of a characteristic peak in an X-ray spectrum is proportional to the concentration of the element in the specific target sample and the number of protons deposited. The particle beam current is the number of (e.g., 3 MeV) protons that hit the surface of the sample per unit of time. If this beam current is integrated over the acquisition time the charge registered is the measure of the number of protons deposited. The number of protons incident on the sample has to be measured in all applications of quantitative PIXE analyses. When the number of counts in a peak area is divided by the measured number of protons a normalised peak area is obtained. This peak area is directly proportional to the concentration of the specific element in the sample in question.

If the target is thin, the measurement of beam current can be performed by placing a conducting material to stop the protons behind the target. A current proportional to the proton beam current can thus be registered. By integrating this current over the time of irradiation, a measure of the total number of protons on the target is obtained. If the irradiation is performed in air this measurement is complicated by the ionisation of gas molecules (Johansson et al. 1995, Mando 1994).

In PIXE analysis of thick conducting samples, corresponding, direct measurements have been made on the sample. Thin layers of carbon have been evaporated on samples of non-conducting materials to enable this measurement. Measurements of the beam current have also been performed on the extraction foil between the accelerator vacuum and the outer atmosphere. Another method used, in analysis of thick non-conducting samples, is to place a rotating chopper in the beam path and use the X-ray emission from, e.g., nickel plating on the wing as a measure of the beam intensity (Mando 1994). The methods used for beam current measurement in thick target PIXE have generally been found to be more unreliable (Maenhaut 1987).

If you want to analyse non-conducting thick samples, without placing them in a vacuum chamber, the measurement of beam current becomes quite complicated (Mando 1994). To maintain flexibility in PIXE, it is desirable to be able to measure the beam current in a reliable manner that does not depend on the type of sample or any other external factors. The system used for proton beam intensity measurements in the external thick target PIXE analyses at Åbo Akademi is reviewed in chapter 2.

2. EXPERIMENTAL

The availability of a particle accelerator (a MGC-20 cyclotron) has made it possible to establish a Particle Induced X-ray Emission (PIXE) spectrometry activity at the Åbo Akademi University. A general aim in the development work has been to make use of the unique features and possibilities of the PIXE technique as a complement to the large number of well established, wet-chemical analytical methods that are available today. In the following, the equipment, and the methods, used in the PIXE analysis of wood materials are described more in detail. What we have is a set-up for external (in air) thick target PIXE (TTPIXE) which can be used for direct analyses of solid biological materials, or the ashes of these materials, without preceding dissolution.

2.1. The experimental set-up at Åbo Akademi University

2.1.1. The proton beam

The MGC-20 cyclotron at Åbo Akademi University is applied for production of the proton beam used in the analyses. H_2^+-ions are accelerated to a kinetic energy of 6.4 MeV (Dahlbacka and Lindblom 1979) and extracted into the external air through a 7.5 μm Kapton®, polyimide ($C_{22}H_{10}O_5N_2$) foil supported by a graphite collimator with an aperture of 1 mm (supporting paper 2). At the impact on the foil separating vacuum and external air, the H_2^+-ions are immediately dissociated into two 3.2 MeV protons. The energy loss in the foil and the air gap (8 mm) between the foil and the target surface is about 0.2 MeV The particle beam incident on the surface of the target sample is thus a 3 MeV proton beam with a diameter of 1 mm (**papers I-VI**). The proton beam forms an angle of 45° with the target surface.

A typical proton beam current used in analysis of thick biological samples is of around 7 nA. A total charge of about 4 μC is thus deposited in the sample during 10 minutes of irradiation. The corresponding beam density of the proton beam is 900 nA/cm^2. In analysis of ashes sufficient counting statistics is obtained using a lower beam current.

2.1.2. Measurement of the proton beam intensity and normalisation of spectra

Solin et al. (1988) developed a device for measuring particle beam intensities in PIXE analyses carried out in vacuum. The device consisted of a small, thin-windowed gas cell through which the particle beam passed before hitting the sample in the irradiation position. Light emission from high purity gas was found proportional to the intensity of the particle beam.

In the present PIXE set-up at Åbo Akademi University (**papers I-VI**), the air in the beam path between the target and the foil separating the beam-line vacuum from the laboratory atmosphere is used as the source of light emission (supporting paper 2). Light induced by the

proton beam is detected with a photo multiplicator (PM) tube. The intensity of the light emitted from the air gap (mainly from molecular band transitions of nitrogen, N_2) is proportional to the intensity of the proton beam. When the current from the PM-tube is integrated over the data acquisition time, an indirect measure of the amount of charge reaching the sample surface is obtained. In quantitative analysis, the areas of element peaks in the corresponding spectrum are divided with this integrated charge from the PM-tube (Q_{PM}). This method used for normalisation of yields (**papers I-VI**) is independent of the sample, and problems related to the ionisation of air, experienced when direct measurements of charge are applied, can be avoided.

Lill (1999a) performed measurements where he obtained a ratio of 210 between the integrated current from the PM-tube and the integrated current from a faraday-cup placed in the sample position. The absolute amount of charge on a sample can be calculated from the integrated charge from the PM-tube using this quotient.

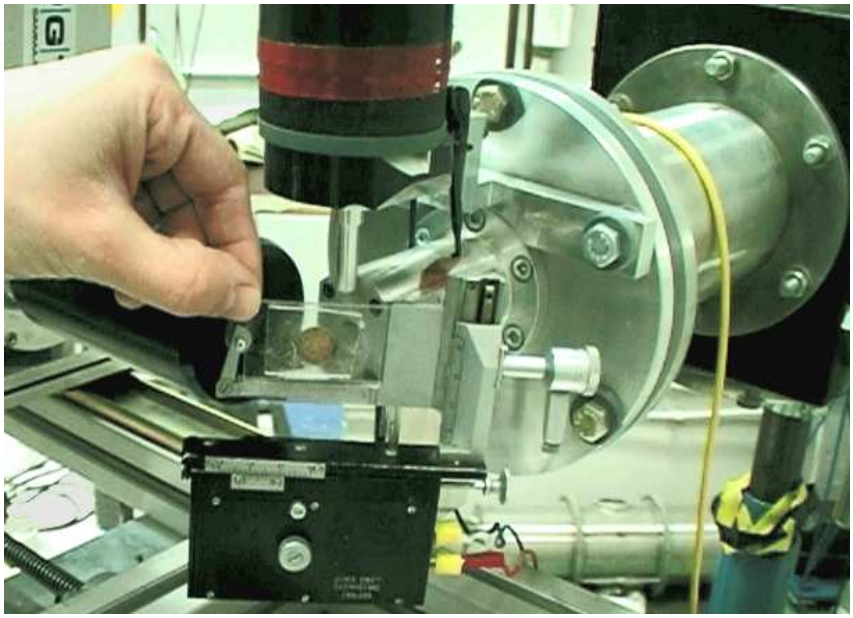

Figure 4. The author is placing a target sample (the pellet in the frame) in position for irradiation. The collimated proton beam is extracted out of the cyclotron vacuum through the beam exit window seen close to the right behind the pellet. The X-ray detector is seen on the left (black exterior, detector window behind finger tips). The PM-tube (top) detects light, induced by protons in the air gap between the beam exit window and the surface of the sample during irradiation.

2.1.3. X-ray detection and spectrum analysis

A maximizing of the detector collection efficiency is achieved by having the maximum possible solid angle of detection (Johansson et al. 1995), by placing the detector as close to the target sample as possible. In the present set-up a so called IGP detector (*Intrinsic Germanium Planar,* from Princeton Gamma-Tech), is used. The detector window (25 μm beryllium) is positioned 38 mm from the irradiated sample surface. The detector and the particle beam form an angle of 90°. Compared to the often used Si(Li) detector, the germanium detector is more sensitive for detection of photons of higher energies (from heavier elements). Even the detection of gamma radiation from a nuclear reaction by the fluorine isotope ^{19}F, with the emission line at 109.89 keV, is possible. However, in the low-energy region (< 2 keV) the sensitivity of the IGP detector, with its 25 μm thick beryllium window, decreases more rapidly (Lill 1999b).

Nowadays there exists a variety of software for spectrum fitting and handling of the data (Johansson et al. 1995). Peak areas representing characteristic emission from elements in the sample are separated from the spectral background and quantified. The quantitative measure of a peak area is the total number of events registered (counts) in the consecutive channels forming a peak in the spectrum. The computer program SAMPO90 (MicroSAMPO version) (Aarnio et al. 1988) was mainly used in earlier work (**papers I-IV**), but in later work (**paper V**) GUPIX software (Maxwell et al. 1989) has been used.

2.1.4. The X-ray absorber

Spectral background, i.e. continuous and unspecific X-ray emission, is mainly bremsstrahlung which is dominating at lower energies in a PIXE spectrum. Without any other absorbing materials than the 25 μm thick beryllium window of the detector between the sample and the detector crystal, the clearly highest yields for elements in wood materials are also seen in this energy region of the spectrum (potassium with the K_α line at 3.35 keV, and calcium with the K_β line at 4.05 keV).

The concentrations of potassium and calcium are generally so high that they can properly be detected even with an additional discrimination of the spectral region where their characteristic emission lines appear (Pallon and Malmqvist 1981). This is especially relevant for ashes of wood materials. By this action, better statistics can be obtained for some heavier elements (metals) appearing at trace element levels.

In the attached **papers II-VI,** a so called "funny filter", a 3 mm thick polycarbonate absorber with a pin-hole, is used. The polycarbonate suppresses radiation in the lower energy region of the spectrum. The drilled hole (0.5 mm diameter) in the filter allows a part of the X-rays emitted towards the detector to reach the detector crystal without encountering absorbing polycarbonate. The funny filter thus allows a more efficient detection of some interesting, heavier, trace elements together with lighter elements of high concentrations, when only one detector is used.

Soft X-rays that are not originating from the irradiated spot of the sample are efficiently absorbed by the funny filter.

2.2. Preparation of wood samples for PIXE analysis

All stem wood and bark samples studied were prepared to thick target samples for PIXE analysis. In TTPIXE analyses a flat surface of the target sample should face the particle beam (Campbell and Cookson 1984). All target surfaces should be placed in exactly the same position so that a reproducible geometry (particle beam – target – detector) is maintained.

Samples of powdered material (certified biological reference materials, ashes etc) were prepared to pellets using a pelleting device. In order to maintain the standard geometry the pellets were prepared according to a standardised method (**papers I-VI**), presented more in detail in section 2.2.2.

2.2.1. Amount of material in a ”thick” target

A study on the distances the 3 MeV protons travel in some prepared target materials is presented in this section. Weighed amounts of the 4 materials listed below were placed in the pelleting device (13 mm diameter) and 4 tons was applied on the piston. The pressure used is the same as in the final step in the normal preparation of target pellets (section 2.2.2.). The thicknesses of the obtained pellets were measured and the densities were calculated.

The computer program TRIM95 (Ziegler, Ziegler et al. 1985) can be used for the calculation of ranges travelled by protons of different energies in materials of different composition. The atomic-% of 1-5 main elements of the matrix, as well as the density of the material, are read into the program.

The materials studied were:

1. Graphite powder (Powdered Graphite, briquetting grade 74 μm, Chemplex Industries Inc. U.S.A.), 100% carbon.
2. Starch, $(C_6H_{10}O_5)_n$, (p.a. from Merck) , atomic percentages: 28.6 % C, 47.6 % H and 23.8 % O
3. Wood Fuel Reference Material, NJV 94-5, from Swedish University of Agricultural Sciences, Umeå, Sweden. Information values for C and H are 51 and 6.04 weight-% respectively (all expressed on dry matter basis). The rest of the matrix was assumed to be O (the certified value for the ash content was 1.22 %) and the atomic percentages calculated were C: H: O = 32.8 : 46.5 : 20.7.
4. Ashes of pine wood. Pine wood was dry ashed at 550°C. The main ash forming elements are potassium and calcium, and these, together with oxygen, constitute the bulk of the ash residue. As the program TRIM95 accepts atomic percentages for 5 elements, values for P and Mg, obtained from own analyses (supporting paper 10), were also included. Weight percentages for K (20 %), Ca (23 %), P (2 %), Mg (4 %) and O (51 %, assumed to constitute the rest of the mass) were used in calculations of atomic percentages for the ash matrix.

The ranges obtained with TRIM95 for the 3 MeV protons, in pellets of the materials listed above, are given in Table 1. The range given is the depth reached by protons in a beam perpendicular to the surface. In the setup used the angle between the sample surface and the

proton beam is 45°, and the depth is thus actually less (depth = range x sin 45°, given within brackets). The detector / sample surface -angle is also 45° and the range is thus also the theoretical maximum distance a photon can travel in the sample material in direction towards the detector.

Table 1. The range of 3 MeV protons in pellets of different materials.

Material	density (g/cm^3)	range(depth) (μm)	mass passed through by protons (mg/cm^2)
graphite powder	2.14	77.5 (54.8)	16.5
starch	1.39	111 (78)	15.4
Wood Fuel	1.13	136 (95.9)	15.4
ashes of pine wood	1.88	104 (73.5)	19.6
air (at STP)	0.00125	139270	17.4

In the last column the maximum amount of material passed through by 1 cm^2 of particle beam is given. It can be seen that the amount of material needed, to prepare a sample that constitutes a thick target, is very small. The ashed pine wood had an ash content of 0.302 %. The amount of ashes needed for preparation of a uniformly thick target, with a surface of 1 cm^2, can thus be obtained from about 6-7 g of the dry pine wood.

The ionisation cross-section for an element decreases with decreasing energy of protons. At the same time attenuation of photons from deeper inside the sample will increase. This means that the detected analytical signal (number of characteristic X-rays reaching the detector) is mainly from a thinner section of the sample than that penetrated by the incoming protons. Only very small amounts of sample material are needed for the TTPIXE analyses. This is a fact that in many cases can be considered an advantage of the method. In bulk analyses of, for example, wood materials, however, the same fact increases the importance of sample preparation that gives target samples that are truly representative of the material to be studied.

2.2.2. Preparation of target pellets

Biological (powdered and homogenised) samples were pressed to pellets with a diameter of 13 mm, using a commercial pelleting device. To obtain pellets with uniform thicknesses, and thus a reproducible measuring geometry, the following “sandwich” technique was used consistently:

- First a larger, standardised amount of graphite powder (0.4 g) is compressed in the pelleting device.
- After this the piston is removed and a small amount of the sample material is placed in the centre on the loosely compressed graphite pellet. A high pressure (4 tons on the piston) is then applied to obtain the final composite target with sample material on the front surface.

The composite pellet is finally placed in a drilled hole, with the same diameter as the pellet, in a piece of plastic board (Fig. 5) with an attached backing. This target preparation technique also enables easy removal of the sample material from the (spectroscopically pure) graphite,

after PIXE analysis, for possible further wet-chemical analysis. Such complementary analysis could be performed to verify the presence of an element in a sample, or, for comparison or calibration in analyses of, for example, small clinical samples (supporting papers 1 and 2). The size of the frame is adapted to fit into the mechanism for moving the target in front of the proton beam (Fig. 4 in section 2.1.2.).

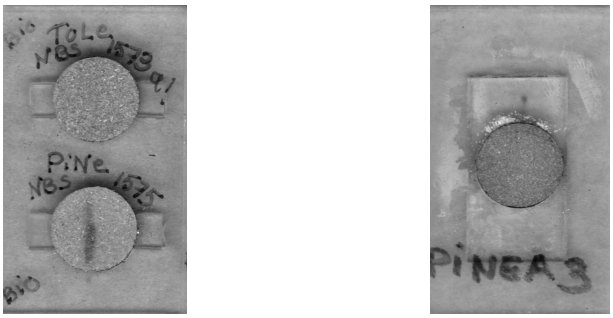

Figure 5. On the left: two biological materials, prepared to target pellets according to the description above. Notice the visible tracks of the proton beam in the lower, irradiated target pellet. On the right is an irradiated target pellet prepared from ashes obtained from dry ashing of the same material (Pine Needles SRM-1575 from NIST, former NBS).

2.2.3. Direct analysis of wood materials

2.2.3.1. Point scans – determination of elemental distributions

For analysis of annual growth rings, pieces of wood are cut out of the log (Fig. 6) or, if sampling a living tree, samples are taken by drilling (**paper I**). The surface is polished and cut plane using a scalpel

By weighing and measuring the density of a piece of dry pine wood was calculated to be 0.7 g/cm^3. In a sample of the same composition as Wood Fuel with a density of 0.7 g/cm^3, protons travel 200 µm (calculation using TRIM95), or approximately 60 µm further than in the compressed, certified standard reference material used for calibration of analysis (compare Table 1). This difference is found acceptable considering the measuring geometry when the distance from the irradiated sample surface to the detector window is 3.8 cm (38000 µm).

Figure 6. A point scan across 5 annual growth rings (heartwood) in a piece of wood to obtain elemental distributions

All spots in a scan are irradiated during the same length of time. The spectrum used in calibration of the instrument is accumulated from a number of spots on a certified biological standard reference material, each irradiated during this same length of time.

2.2.3.2. Effects of the proton irradiation on biological materials

Effects on samples from irradiation with charged particles have been observed especially for so called micro-PIXE (Campbell and Cookson 1984, Cookson 1988, Watt et al. 1988, Themner 1991), where beam diameters of 1-10 μm are used. To maintain this small beam diameter, the analyses have to be performed in high vacuum. The vacuum increases the risks for possible losses of sample material (Räisänen 1992, Räisänen 1989, Martinsson 1987) especially when heating occurs (Martinsson 1987). The beam current density for micro-PIXE is kept relative high, i.e. at levels of 10^7-10^8 nA/cm^2 (Watt et al. 1988, Watt et al. 1997), in order to obtain sufficient statistics from analyses of the very limited surface area.

The processes behind the beam damages are not fully known (Johansson et al. 1995, Lövestam et al. 1990, Hansen et al. 1980) and have not been studied systematically for biological materials, as stated by Watt et al. (1997). Damages have been grouped into two categories: beam damages and effects caused by heating. The first category is related to the total amount of deposited charge, while the latter is related to the intensity of the particle beam. Themner et al. (1990) suggested that the two processes interact when sample mass is lost, i.e. heat evaporates the volatile compounds that are formed as the results of beam damages. Williams (1984) has pointed out the possibility that oxidation may take place in the sample during irradiation in air. Beam effects that occur can considerably complicate the quantification of the analytical results (Cookson 1988, Themner at al. 1990).

The temperature increase in a specific sample is basically dependent on the intensity of the projectile beam, i.e. the beam current (Hansen et al. 1980, Nobiling 1986). The temperature reached during irradiation is a result of an energy balance between the energy deposited on retardation of the protons and the removal of energy through heat radiation as well as heat transfer in the sample and via a possible gas atmosphere (Gloystein and Richter 1987). The beam effects on a sample are thus smaller in external PIXE. Campbell (p. 24 in Johansson et al. 1995) regarded helium as a better coolant than air for sensitive samples because of its better heat transfer capacity. Gloystein et al. (1987) have considered flushing the sample with gas, or placing the sample in an atmosphere of helium, as the only way to obtain efficient cooling of the sample.

Zeng et al. (1990) studied the effects of 2.1 MeV protons on (thin) paper in air. They were able to measure the temperature of the paper and could establish that the temperature rise was less than 5 ˚C if the beam current density was kept below 30 nA/ cm$^{2.}$ Despite this, beam damage in the form of reduced strength and brightness could be noticed after deposition of about 0.4-0.6 μC/cm^2. No reports on measurements of exact temperatures during analyses of thick biological samples have been found. Heat generated in thick samples is though greater because the whole energy content of the particle beam is deposited in the sample (Johansson and Campbell 1988).

When analysing thick biological samples in air with the set-up described in this thesis, visible effects on the sample surfaces are observed (Figs 5 and 6). Therefore a study of these effects on yields was performed where the same spot of a biological material (pellet of the certified reference material Tomato Leaves, SRM 1573 from NIST, former NBS) was irradiated with 3 MeV protons. Separate spectra were registered during 5 consecutive irradiations of the same spot on the sample. A clear enrichment of elements with increasing total charge could be demonstrated (supporting paper 7). For potassium and zinc, the relative standard deviations were 7 and 6 % respectively, due to increasing yields in the consecutive irradiations. A similar test on ashes of the material showed constant normalised yields for all five consecutive spectra. The relative standard deviations (n=5) obtained for potassium and zinc were 1.3 % and 2.9 % respectively (supporting paper 7). The ashes can thus be considered inert. No further loss of sample material occurs during irradiation of ashes in PIXE.

The observed effects of the particle beam on the biological sample targets show the importance of similar beam currents and irradiation times for all samples in the analytical session.

2.2.4. PIXE analysis of dry ashed wood materials – bulk analysis

If the bulk (average) concentration of a material is to be determined, the sample analysed has to be truly representative of this material as a whole. Heterogeneity as well as changes in the composition of the target samples during irradiation are factors that both can affect negatively the quantitative bulk analysis of biological material when ion beam techniques are used (Maenhaut 1987, Valkovic et al. 1995).

2.2.4.1. Dry ashing of biological materials

Representative samples of wood are difficult to prepare due to the heterogeneity of the material (Lövestam et al. 1990). A point scan analysis across 3 annual growth rings in spruce wood was performed in **paper I**. Within this limited area of wood large variations in the concentrations of, for example, Fe (from below the detection limit of 14 mg/kg up to 174 mg/kg), Cu (3-33 mg/kg), K (200-930 mg/kg), Mn (17-58 mg/kg), Ca (600-2200 mg/kg), Sr (5-15 mg/kg), and Zn (9-25 mg/kg) were observed.

The organic matrix of a biological sample is removed during dry ashing. In the residue, the ash, the ash forming elements are transformed to oxides or, in various extents, to carbonate forms (Mader et al. 1997, Hoenig 2001). The ash content of birch, pine and spruce wood is low, or around 0.2-0.4 % of the dry weight. For this kind of materials a strong enrichment of the ash forming elements is obtained. The ashes can be homogenised for analysis by shaking, to represent a large amount of the original biological sample material.

The choice of ashing temperature should, according to Hoenig (2001): “ensure the quantitative removal of the organic matter without a partial or total loss of analytes by volatilisation or their incorporation into a residue insoluble in usual reagents”. Hoenig (2003) also stated that losses reported as being due to volatilisation are often, in reality, due to

retention problems. Koh et al (1999) studied losses of the elements occurring in stem wood from trees heated in an open vessel in a muffle furnace, using instrumental neutron activation analyses (INAA). No losses of Mn, Ca, Sr, Ba Fe, Cu and Zn were observed at temperatures up to 600 °C. K and Rb concentrations decreased slightly at 600 °C, but no losses were observed at 550 °C. Llorente and Garcia (2005) dry ashed lignocellulosic biomasses, including pine chips, at different temperatures and ended up recommending dry ashing temperatures of 500-550 °C. They observed no decreasing trend for the recoveries of the elements Ca, K, Na, S, P, Si, Al, Fe, Ti, Ba Mn Sr and Zn, when dry ashing pine wood at 400, 500, 550 and 600 °C. The amounts of S, Na, Al and Fe in the original biomasses were, however, found to be somewhat higher than in the ashes. Azcue and Mudroch (1997) presented a study where they ended up recommending dry ashing at 550 °C for determination of Cd, Co, Cu, Fe Mn, Ni Pb and Zn in vegetation. Väisänen et al. (2008) dry ashed a certified standard reference material of pine needles at 500 ˚C with no observed losses of Al, Ca, Cu, Fe, K, Mg, Mn, Na, Zn and P. According to Bock (1979), temperatures up to 800 °C can be used in dry ashing of biological materials, still with full recovery of phosphorus.

Salts of alkali and alkaline earth metal ions have been used as “ashing aids” in dry ashing prior to determination of sulphur in organic materials. (Bock 1979). Our own experience from dry ashing of Tomato Leaves at 550 °C (**paper II**) is that sulphur is almost quantitatively retained in the ash. However, in the PIXE spectrum for ashes of Bovine Liver, no peak for sulphur was found, although the content of sulphur in the ash would have been over 18 weight %, if fully retained during dry ashing.

From the reported certified concentrations for the Tomato Leaves CRM, and knowing the ash content, the composition of the ash residue after ashing at 550 °C can be calculated to be (compare appendix 1): 23 % K, 15 % Ca and 1.8 % P. For ashes of Bovine Liver the corresponding calculated numbers are: 23 % K, 0.27 % Ca and 26 % P. According to Obernberger (1998) test runs and evaluation of material balances showed that up to 90% of the sulphur in a biofuel can be bound in the ashes from combustion of the material. S-fixation efficiency (Obernberger 1998) in the ash depends on the concentration of alkaline earths (especially Ca). In the case of bovine liver and similar materials, with a high content of phosphorus, the binding of cations in phosphates can also hinder the sulfation process.

Concentrations of sulphur are also reported in the present work. Bark and wood samples have a relatively similar composition of the main elements. The Ca/S ratio is high, and phosphorus concentrations are relatively low. In the calibration procedure for the bulk analyses, biological, certified reference material, of closely matching composition of mineral elements, are dry ashed in the same way as the samples.

Ashes from dry ashing of biological material can be dissolved in acids and pipetted on to foils, which can be analysed as thin targets with PIXE (Malmqvist 1990). In Thick Target PIXE no digestion of the ashes is performed and therefore problems caused by incomplete dissolutions, or crystallisations forming locally thick segments (Pallon and Malmqvist 1981), can be avoided.

Due to the enrichment of analyte elements in ashes a lower beam current is needed to obtain sufficient statistics for characteristic X-rays. A lower beam current will also mean that induced spectral background from, for example, the air or the exit window is less.

A drawback of dry ashing is the loss of some volatile elements like, for example, halogens. Dry ashing of some types of biological samples can also give ashes that contain high concentrations of elements that will produce a high spectral background in the PIXE spectrum through intense emission of gamma-radiation. An example is the high content of sodium in ashes of blood plasma, which strongly diminishes the gain of enrichment by ashing (Pallon and Malmqvist 1981). The levels of sodium are, however, low in wood materials (supporting paper 10, see also Table 12 in this thesis).

A concept for bulk analysis of wood materials, including classical dry ashing and direct PIXE analysis of the ashes as thick targets, was developed in **papers II-III**. Samples, as well as the certified biological reference materials used for calibration (see section 2.3) were dry ashed at 550 °C. Dry ashing was performed in a programmable furnace which enables processing samples in a reproducible manner. The temperature was increased slowly, especially during the carbonisation step, to avoid local hot spots or self ignition. The biological materials were dry ashed in open crucibles and the residue, the ashes, were homogenised by shaking. The method is especially favourable for the analyses of heavier elements at trace level concentrations in materials with low ash content, wood being one example. Another application has been the analyses of honey samples (supporting paper 6).

The European committee for standardisation has published a standard method for the determination of ash content in solid bio fuels (CEN/TS 14775) where the temperature to be used is 550±10 ˚C. This standard is planned to be upgraded to a full formal European standard which would then replace existing national standards. The concept presented in this thesis enables direct analyses of, for example, heavy metals in ashes of biofuels and should be of potential interest when further studies of ash residues are considered.

2.2.4.2. The chemical composition of some dry ashed reference materials

In appendix 1 the certified concentrations, and in some cases also concentrations given for information only, are listed for some CRMs available. The elemental concentrations in the ashes were calculated using the ash contents obtained from dry ashing of the biological materials at 550 ˚C. A biological certified standard reference material (CRM), which is to be dry ashed and used in calibration, should have the elemental concentrations well certified and the concentrations in the ash should clearly exceed the limit of detection for the elements to be quantified. The CRM Pine Needles 1575 from NIST (National Institute of Science and Technology, Gaithersburg, MA, USA) meets the criteria mentioned for most elements (including phosphor and trace metals) normally quantifiable in the bark and wood samples analysed. The elemental concentrations certified are also in agreement with the comprehensive compilation of literature data for this CRM as reported by Roelandts and Gladney (1998), which was not the case for the concentration of iron in Tomato Leaves (certified to 690±25 mg/kg). For this CRM Roelandts and Gladney (1998) report a mean concentration of 600 mg/kg for 68 published analyses of Fe. This corresponds to a concentration of 3.09 mg/kg in the ash, which is also in agreement with our own result (3.00 mg/kg of dry ash, **paper II**). The data compiled by Roelandts and Gladney (1998) were also used to complete appendix 1.

Calculated elemental concentrations in the ash of the Pine Needles CRM, as well as in ashes of two other reference materials used in the calibration and evaluation of analyses of stem bark and wood, are summed up in Table 2. The two other CRMs included in the table are Wood Fuel (Pine) NJV 94-5, a mix of 30 % pine wood chips and 70 % pine bark, and Energy Forest (Salix) NJV 94-3, both from the Swedish university of Agricultural Sciences, Umeå. Concentrations of chlorine and bromine are included in the sums although these elements are expected to be almost quantitatively lost at 550 ˚C, chlorine already at temperatures > 250 ˚C and bromine at temperatures > 400 ˚C (supporting paper 14).

Calculated concentrations of corresponding oxides are also included in Table 2 and summed up. A clear anti-correlation between the calcium concentrations and the total contents of oxides was found (r = -0.9998, n=3), and the mass lacking (100% - total % of oxides) was assumed to be the CO_2 in carbonates. The concentrations of carbonate carbon as well as the oxygen concentrations (100% -% carbon –% ash forming elements) were calculated and included in the table. Oxygen is clearly the dominating element in the ashes, followed by calcium and potassium. These three elements together constitute ¾ of the total mass.

Table 2. Concentrations of elements and their oxides in ashes of some wood based CRMs, calculated from certified concentrations, as well as from consensus values by Roelandts and Gladney (1998), and the ash contents (ash %) obtained by dry ashing at 550 ˚C. The concentrations of (carbonate) carbon and oxygen are estimated by calculation (see text).

	Energy Forest		Pine Needles		Wood Fuel	
ash%	1.57		2.52		1.23	
	element [mg/kg]	oxide [%]	element [mg/kg]	oxide [%]	element [mg/kg]	oxide [%]
Ca/CaO	280000	39.2	163000	22.8	284000	39.7
K/K_2O	127000	15.3	147000	17.7	73000	8.79
P/P_2O_5	32000	7.33	48000	11.0	17000	3.90
Mg /MgO	21600	3.58	46800	7.76	24300	4.03
Si/SiO_2	7630	1.63	51200	11.0	18700	4.00
Al/Al_2O_3	1300	0.246	22000	4.16	21100	3.99
Mn/MnO	3800	0.491	26800	3.46	17000	2.20
Fe/Fe_2O_3	1650	0.236	7900	1.13	5700	0.815
Na/Na_2O	1840	0.248	1400	0.189	3200	0.431
Zn/ZnO	4770	0.594	2600	0.324	3080	0.383
Rb/Rb_2O			464	0.102		
Sr/SrO			190	0.023		
Pb/PbO	8.90	0.010	429	0.468	55.2	0.060
Cu/CuO	254	0.032	120	0.015	180	0.023
Ni/NiO			110	0.014		
Cr/Cr_2O_3			100	0.018	65.0	0.012
Cd /CdO	114	0.013	8.30	0.001	21.9	0.003
Cl	6360	0.636	11800	1.17	8110	0.81
Br			300	0.03		
Ti/TiO_2					195	0.033
S/SO_3	16500	4.12	49600	12.4	15000	3.75
Total %	50.5	73.7	58.0	93.7	49.1	73.0
CO_2 %		26.3		6.28		27.0
C %		7.2		1.71		7.4
O %		42.3		40.3		43.6

2.3. Calibration of the PIXE analyses of stem wood and bark

The expression $I(Z)=f(C_z, ME, IE)$ has been used to describe the factors affecting the detectable intensity of X-rays emitted from an element (atomic number Z) in a thick sample (Campbell et al. 1993). The expression indicates that the intensity is dependent on the concentration (C_z) of the element as well as on the matrix effects (ME), i.e. effects of other elements than Z on I(Z). The intensity is also dependent on the instrumentation (IE) used.

If samples of the same type are irradiated, using the same set-up, the normalised yields can be directly used in a comparison of concentrations. Absolute concentrations can be obtained by using a matching standard (certified standard reference materials) with known concentrations of the elements to be quantified. The exact matrix and instrumental effects do not have to be known in order to perform this calibration.

Clayton (1987) compared the theoretical X-ray yields from elements in thick samples of several kinds of biological materials. Reported contents of C, H and N for the different materials were used in the calculations and oxygen (O) was assumed to constitute the rest of the sample masses. For elements in the range P to Ca, matrix effects caused differences in yields of up to 20 %. For elements heavier than potassium the variations were within ± 5% for the different biological materials. When the samples were grouped into animal (blood, fish, bovine liver and lung) and plant material (pine needles, leafs, spinach, tomato leaves and cellulose) the variations in yields within the respective groups were found to be at maximum 10 % for the elements P – Ca, i.e. the matrix effects are relatively small.

Similar comparisons of matrix effects are made in **paper II** for ashes obtainable from dry ashing of different types of biological materials. The compositions of ashes of some vegetables, meat and edible bowels are calculated from the reported elemental and ash contents of the materials. Ashes of the certified biological reference materials Tomato Leaves, Pine Needles and Bovine Liver (from the National Bureaus of standards, NBS) are also included. The matrix effects are found to be small for elements heavier than calcium. The strongest matrix effects for ashes of Pine Needles (**paper II**) are seen for calcium, comparing to ashes of vegetable foods. The content of potassium is clearly the highest in the ashes of vegetable foods, and the K: Ca ratio is roughly 10:1. In the ashes of Pine Needles the K: Ca ratio is about 1:1 giving clearly lower attenuation of the X-rays from calcium. A positive error of over 40 % was predicted for calcium if an ash of the former type would be used in calibration of the PIXE analysis of the ash of pine needles. However, it was shown that calibration using a biological material of similar origin as the samples keeps the matrix effects, for all the detected elements, within acceptable levels. In this thesis the dry ashed Pine Needles standard reference material has been used in calibration of the analyses of dry ashed stem wood and bark samples.

In PIXE analyses the stopping range of the protons in the target sample is relatively short. The amount of material needed for a TTPIXE analysis is thus small. However, the demands on homogeneity of the analysed material are great (Valkovic et al. 1995) when representative results are to be obtained in bulk analyses. In the attached **papers I-VI** calibration and evaluation of the analyses are performed using certified biological standard reference materials (CRMs). The bulk analyses of stem bark and wood are performed by: dry ashing the biological material, homogenising the ashes by shaking and pressing the ashes to pellets that are analysed by PIXE. Dry ashed biological CRMs are used in the calibration process (**papers II-VI**).

Yields from samples are compared with the yields from the CRMs, or the dry ashed CRMs, of known concentrations. All conditions, the measuring geometry and all instrumental parameters, are kept constant during the analytical session. On this basis a calibration constant, K_z, can be calculated for each element with a certified concentration in the CRM that yields a large enough peak in the obtained PIXE spectrum.

The calibration constant K_z gives the number of characteristic X-rays registered when a target sample with a known concentration (C_Z) of the element is irradiated with a certain number of protons. The measure of deposited charge used in the present set-up is the integrated current from the PM-tube, denoted by $Q_{PM.}$ A calibration constant can thus be calculated using the formula:

$$K_Z = \frac{Y_Z}{C_Z . Q_{PM}} \qquad (12)$$

During acquisition of a spectrum the intensity of the proton beam is kept at a level that gives the detection system the time to register all the incoming photons. If the detector is blocked, so called dead-time appears. When, for example, 2 % of the real time is dead time the yields of the elements have to be divided by the factor 0.98.

The constant K_z enables the quantification of the concentration (C_{ZS}) of the corresponding element in a sample of similar type. If Y_{ZS} is the count of the characteristic X-rays from the sample, and the measure of protons incident on the sample is $Q_{PMS,}$ the concentration in the sample (Czs) can be calculated as:

$$C_{ZS} = \frac{Y_{ZS}}{K_Z Q_{PMS}} \qquad (13)$$

2.4. Limits of detection

The limit of detection, LOD, for an element was determined according to general practice in PIXE (Maenhaut and Malmqvist 1992). The square root of the background intensity in the spectral interval of the principal X-ray line was multiplied by 3 and this product was transformed into a concentration value by dividing it with the calibration constant. The spectral background intensity was obtained with the computer program MicroSAMPO version 3.1 (Aarnio et al. 1988).

The two first columns of concentration values in Table 3 give the detection limits that were reached for a spruce and a pine wood sample, respectively, when the PIXE analyses were performed on thick targets of the (enriched) dry ashed materials. The two series of LODs reflect the similarities of the spectral backgrounds from the two ashes (the ash contents were identical). These detection limits are dependent on the detection limits for the elements in the irradiated samples (the ashes) and the enrichment in the ashing procedure. The LODs for the ashes of wood are given in the third column as a mean of the LODs obtained from the two spectra. GUPIX software (Maxwell et el. 1989) was used to obtain the last column with LODs for direct PIXE analysis of the biological material.

The limit of quantification, LOQ, is generally related to a signal of 10 times the square root of the spectral background. The LOQs can thus be obtained by multiplying the concentration values in table 3 by a factor of 10/3.

By comparing the two last columns in Table 3 it can be seen that the heavier ash matrix is more unfavourable, and detection limits are higher for the ash than for the biological material. However, a higher detection limit for the ash matrix is clearly compensated by the strong enrichment of the elements retained in the ashes of the wood materials. From Table 3 it can be seen that in a direct analyses of wood the detection limit for copper is approx. 1.4 mg/kg, and the limit of quantification is thus above 4 mg/kg of dry wood. The detection limit for copper in the ashes of wood is approx. 9 mg/kg, while the enrichment factor obtained in the dry ashing of both wood samples in Table 3 is 100 / 0.331 = 302. Dry ashing for PIXE analysis thus enables quantification of copper down to concentrations of 0.1 mg/kg in the original wood samples. Bulk concentrations of copper were found to be around 1 mg/kg in wood analysed in this thesis (**paper VI**).

Table 3. Limits of detection (LODs) reached for spruce and pine wood samples respectively (supporting paper 7) when the samples are enriched by dry ashing (ash contents of both samples were 0.331 wt-%) for TTPIXE analyses, the LODs for the wood ashes, and the LODs for direct analyses of the pine wood. All concentrations are in mg/kg of respective dry material.

		Limits of detection			
Line	Energy (keV)	spruce	pine	wood ashes	pine wood
Si (Kα)	1.77		82	25000	5200
P(Kα)	2	16	15	4700	510
S(Kα)	2.34	14	13	4100	130
Cl(Kα)	2.66				81
K(Kα)	3.35	1.2	1.1	350	34
K(Kβ)	3.58	6.4	5.6	1800	
Ca(Kα)	3.71	1.3	1.1	360	
Ca(Kβ)	4.05	6.2	5.7	1800	22
Mn(Kα)	5.91	0.22	0.24	70	7
Fe(Kα)	6.39	0.11	0.12	35	9
Mn(Kβ)	6.49	0.85	0.92	270	
Fe(Kβ)	7.04	0.33	0.37	110	14
Ni(Kα)	7.41	0.06	0.07	20	2
Cu(Kα)	8.04	0.03	0.03	9	1.4
Zn(Kα)	8.63	0.02	0.03	8	1
Cu(Kβ)	8.85	0.16	0.21	56	
Zn(Kβ)	9.58	0.1	0.12	33	
Pb(Lα)	10.54	0.05	0.06	17	3.3
Br(Kα)	11.84				1.5
Pb(Lβ)	12.62	0.07	0.08	23	
Rb(Kα)	13.36	0.03	0.03	9	1.5
Sr(Kα)	14.14	0.04	0.03	11	1.7
Rb(Kβ1)	14.96	0.18	0.14	48	
Sr(Kβ1)	15.8	0.1	0.08	27	
Ag(Kα2)	21.96	0.23	0.09	48	
Ag(Kα1)	22.14	0.11		33	13
Cd(Kα2)	23.01		0.17	51	16
Ba(Kα2)	31.77	1.1	1.1	330	
Ba(Kα1)	32.14	0.63	0.64	190	81
Ba(Kβ1)	36.33	1.6	1.3	440	
F-19	109.89	0.14	0.16	45	

The preparation of target samples from the dry ashed wood material thus gives two major benefits: The ash can be homogenised by shaking to obtain a more homogeneous and representative sample to be analysed by PIXE. This is of utmost importance in bulk analysis. At the same time the enrichment of elements in the ash enables the quantification of some additional trace elements in the wood material.

3. ANALYSIS OF STEM WOOD AND BARK

3.1. Macroscopic structure of the stem of a tree.

The main parts that can be seen in a cross section of a tree stem are shown in Fig. 7, and are further described in the text below.

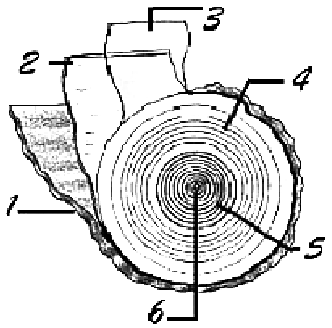

Figure 7. Schematic structure of a tree stem

1. The **outer bark** (rhytidome) is dead tissue that protects the stem from mechanical injury and excessive evaporation (Raunemaa et al. 1987, Poikolainen 1997). It is continuously renewed from inside and also insulates the tree against cold and heat.
2. The living **inner bark** (phloem) is the pipeline for transportation of the sap which carries assimilates from the leaves in a downward flow (Fengel&Wegener 1984). The outermost phloem tissue gradually changes to rhytidome to become a part of the protective cover of the stem.
3. The growth layer, **the cambium,** is a very thin layer of living cells between wood (also called xylem) and the inner bark (phloem). In this layer cell division takes place, producing phloem on the outside and sapwood on the inside.
4. The xylem/wood closer to the cambium, which contains living cells and conducts water and minerals nutrients from the roots up to the foliage of the tree, is called **sapwood**. As the tree gets older the innermost cells of sapwood loose their vitality and turn into heartwood.
5. Heartwood is the central pillar of the stem which consists of older and dead cells. This inner part of the stem (dark-coloured in for example pine) provides structural strength. When sapwood has begun to change to heartwood, the proportion of heartwood will increases during the lifetime of the tree (Kozlowski and Pallardy 1997). In this process pigments as well as phenolic substances and resins are formed (Sjöström 1992). As a result of this process the heartwood is practically impermeable to water. A zone close to the pith, produced by the young cambium, is named juvenile wood.
6. The pith represents the tissue formed during the first year of radial growth and is seen as a dark spot in the middle of a disc of stem wood (Sjöström 1992).

Each year the trees form new wood increments in their radial growth. In Nordic countries the growth of trees is stopped during the cold winter to start again with a rapid growth in early spring/summer forming **earlywood**. Later in summer the growth is slowed down. During the evolvement from earlywood to **latewood** the cell diameter becomes smaller while the cell walls become thicker (Fengel&Wegener 1984). The **latewood** is seen as darker wood outside

the lighter earlywood in, for example, pine and spruce. The earlywood and the latewood together form an **annual growth ring**, also named year ring or tree ring. A tree ring constitutes the wood produced during a specific growth season. The earlywood part of sapwood predominantly conducts the water and mineral elements within the tree (Fengel&Wegener 1984). In this context it should be mentioned that, according to Kozlowski and Pallardy (1997), elements essential for the growth of woody plants include the macronutrients N, P, Ca, Mg and S, and the micronutrients Fe, Mn, Zn, Cu, B, Mo and Cl.

3.2. Tree species sampled and sampling sites

Stem bark and wood samples of birch (Silver birch, *Betula pendula*), pine (Scots pine, *Pinus sylvestris L.*) and spruce (Norway spruce, *Picea abies*), the main tree species in Finland, were analysed for their elemental concentrations. The trees sampled were from different sites in mid-western (the region of Ostrobothnia) and south-western Finland. Some main sites are marked in the map in Fig. 8.

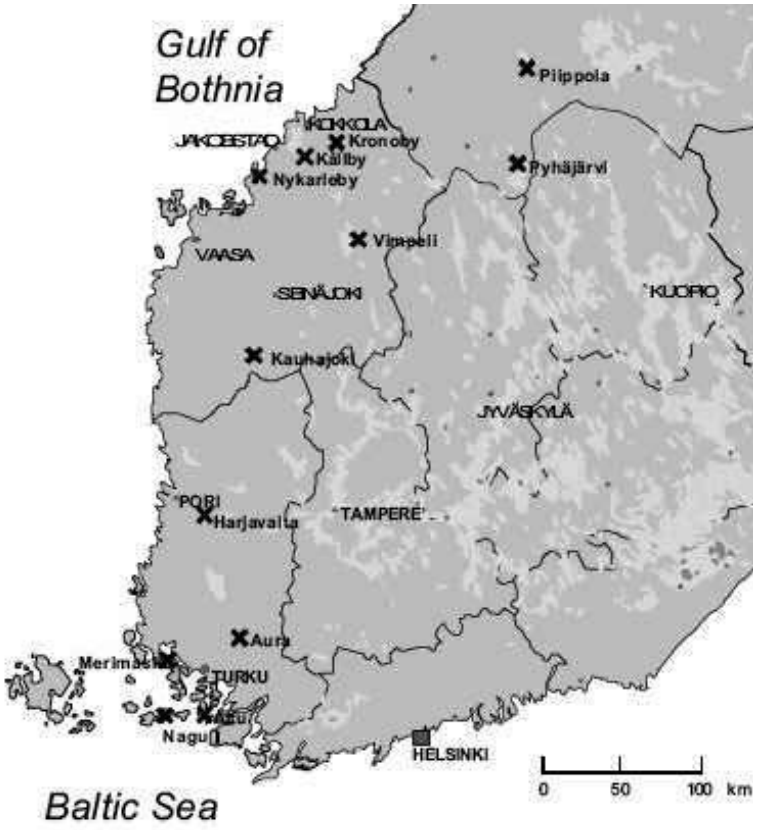

Figure 8. Map showing sampling sites in Finland (**paper VI**).

3.3. Radial distribution of elements in stem wood

3.3.1. Distribution of elements from pith to bark in a disc of pine wood

Stem wood of pine was sampled during forest felling in the late winter of 1995 at Aura in south-western Finland (Fig. 8). A piece of stem of diameter 15 cm (the minimum allowed diameter for pine log) was cut from the leftover top/crown part of a pine tree. A pillar of wood was cut out from a thin disc of this pine stem wood (Fig. 9). The number of annual growth ring in the disc (the pith age) was counted to 50. The pillar was divided into 5 mm thick pieces. The pieces of wood were placed in frames for PIXE analysis. Then spots on the plane cut target surfaces were irradiated during 1 minute each. The first target sample included the pith, while the following samples represented wood at 5 mm, 10 mm, 15 mm etc. out from the pith. The last analysis was made on outermost wood from close to the bark.

Figure 9. The radially sampled disc of pine stemwood from Aura. The dashed lines indicate the position of the wood analysed in the cut out pillar. The scale gives the distance to the pith in mm. The needle indicates the border between heartwood and sapwood, at about 30 mm out from the pith.

In Fig. 10 the concentrations of Ca, Zn, Mn and K at the increasing distances from the pith in the pine wood disc in Fig. 9 are shown. Notice the magnification of the concentrations of zinc (x 15) and the demagnifications of the concentrations of calcium (/ 9) and potassium (/ 3). This scaling is done to properly fit all profiles into the same diagram in order to enable better visual comparison of trends.

It can be seen From Fig. 10 that concentrations of Ca, Mn and Zn are clearly higher in the wood closest to the pith. The elements are, however, relatively evenly distributed in the rest of the wood. A continuous decreasing trend is seen for calcium and manganese towards the bark of the stem. Linear fits to the concentrations of Ca and Mn in wood 5 -75 mm out from the pith gave the following equations: $C_{Ca} = 1597 - 12.5 \cdot x$ *and* $C_{Mn} = 172 - 1.23 \cdot x$, where the concentrations are in mg/kg and x is the distance from the pith in millimetres.

The concentrations of zinc are relatively evenly distributed within the heartwood outside of the pith region (5-30 mm). For calcium, and especially for zinc, a distinct decrease in concentrations is seen passing from heartwood to sapwood. The lowest concentrations of zinc in the pine stemwood are found in the innermost sapwood, at 35-40 mm from the pith, outside of which an increasing trend can be observed towards the bark. For calcium and manganese a slowly decreasing trend is seen throughout the wood outside the pith.

Potassium shows a quite different concentration pattern. The concentrations in heartwood, as well as in the inner half of the sapwood, are clearly below the mean value reported from analyses of a large number of pine wood samples in **paper VI.** A very steep increase in concentrations is, however, seen in the outer half of the sapwood. A maximum concentration of 1350 mg/kg is reached for potassium in the outermost sapwood analysed.

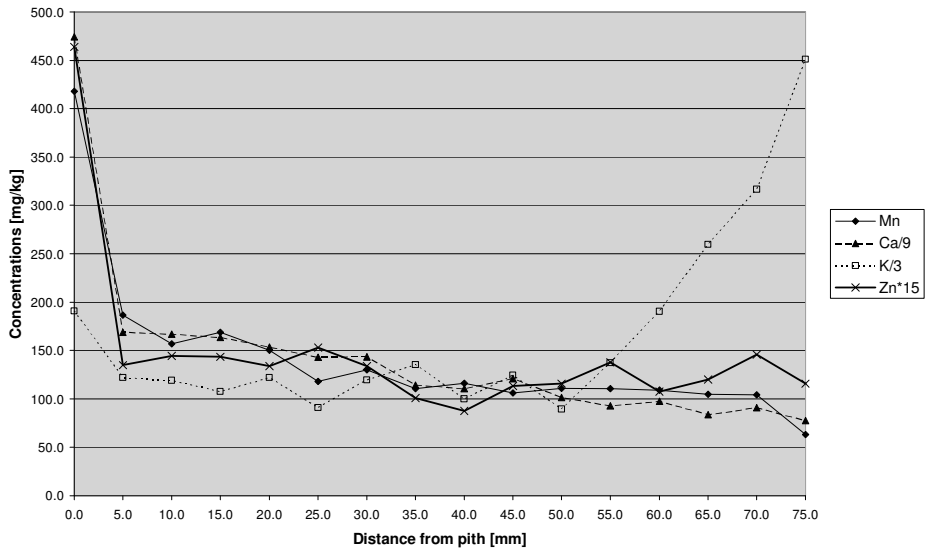

Figure 10. Concentrations of Mn, K, Ca and Zn as function of distance from the pith of the pine wood disc shown in Fig. 9. Scaling of the concentrations is done according to the insert.

Correlation coefficients (r) between the elemental concentrations in heartwood (5-30 mm from the pith) and sapwood (35-75 mm) respectively are given in Table 4 using the Correl-function in Microsoft's Excel™ software. A positive linear correlation is obtained between calcium and manganese, which is especially strong in heartwood. The strongest negative correlation is obtained between potassium and zinc in heartwood. In sapwood, however, the correlation coefficient for the corresponding sets of concentrations ($r_{K\text{-}Zn}$) is positive.

Table 4. Correlations between concentrations of elements obtained from the scan in Fig. 10. The correlation coefficients are given separately for heartwood and sapwood. Wood at 5-30 mm from the pith represents heartwood. Concentration values for the wood including the pith were excluded.

	5-30 mm				35-75 mm			
	K	Ca	Mn	Zn	K	Ca	Mn	Zn
K	1.000				1.000			
Ca	0.438	1.000			**-0.786**	1.000		
Mn	0.542	**0.927**	1.000		**-0.868**	**0.617**	1.000	
Zn	**-0.879**	-0.136	-0.395	1.000	**0.380**	-0.513	-0.149	1.000

The data obtained in the study of the pine stem wood from Aura are summarised in Table 5. It is seen that concentrations of manganese, zinc and calcium are 3-4 times higher close to the pith compared to the mean elemental concentrations (n=15) for wood ≥5 mm outwards from the pith. Mean values from bulk analyses of a large number of pine stem wood samples, from Table 15 in **paper VI**, are also included as the last column in Table 5. Only for potassium, is the mean concentration for the disc of pine wood from Aura lower than the reference value from **paper VI**.

Table 5. Concentrations of elements in wood close to the pith of the pine stem (0 mm), mean values for elemental concentration in wood 5-75 mm out from the pith, and the ratio between the pair of data. The weighted mean elemental concentrations (see text) as well as bulk concentrations obtained from analyses of a large amount of pine stem wood samples (Table 15, **paper VI)** are also included. All concentrations are given in mg/kg of dry wood.

	max 0 mm	mean (n=15) 5-75 mm	quotient	weighted mean	mean (n=37) paper VI
Ca	4300	1100±290	3.9	940	750
Zn	31.0	8.4±1.3	3.7	8.1	7.3
Mn	420	120±31	3.4	110	61
K	570	500±310	1.2	620	625

Elemental concentrations in wood at larger distances from the pith represent a greater amount of the disc of stem wood. To obtain mean values more representative of the bulk of wood in the disc, weighted means were calculated by: allowing concentration values obtained for wood at 5 mm from the pith to represent all wood within this radius. The concentration values for wood at 5 mm from the pith were multiplied by the factor $\pi \cdot 5^2$, the concentration values for wood at 10 mm from the pith were multiplied by ($\pi \cdot 10^2 - \pi \cdot 5^2$) and so on. The sums of the 15 products were finally divided by a factor $\pi \cdot 75^2$. These weighted mean elemental concentrations are included in Table 5.

Concentration values for potassium in wood 5-60 mm from the pith were in the range 269-571 mg/kg, and they were all below the mean value for pine stem wood in **paper VI** (625 mg/kg). A broad concentration interval of 269-1350 mg/kg was thus obtained for potassium in the radial analysis of the pine disc. Calculation of an area weighted mean value resembles better the result to be expected from sectorial sampling of the disc. The concentrations of Ca, Zn, Mn and K found in stem wood at crown height in the pine from Aura can thus be said to be very similar to those found for pine stem wood in **paper VI,** where samples where taken from the lower end of the stems

3.3.2. Point scans across heartwood of pine

3.3.2.1 Scans across the pith and the innermost annual growth rings

Radial point analyses in steps of 1 mm were performed, starting from the pith, to further investigate the distribution of elements in the innermost wood layers of pine stem wood. Wood pieces of the size 2 cm x 3 cm were cut out from the centre of discs of three pine trees from different sites. The samples to be irradiated were fit into the opening of frames with their plane cut surfaces in level with the frame surface.

The first sample scanned, was from the next slice cut from the same piece of pine stem wood from Aura as in the preceding section (Figs 9 and 10). The two other samples scanned were from Turku (the island of Hirvensalo), south-western Finland, and from Jakobstad in mid-western Finland (about 450 km north of Turku). In the two latter cases the discs were cut from the lower end of the trunk. The two trees were felled in late winter (February).

The irradiated sample of pine wood from Aura is shown in Fig. 11. The intention was to register the first spectrum during bombardment of the absolute centre (the pith) of the wood. After this the sample was moved 1 mm and the acquisition of the next spectrum was started. Each spot was irradiated for 8 minutes. The 15 point scan was performed in the same radial direction as the analyses presented in Fig. 10.

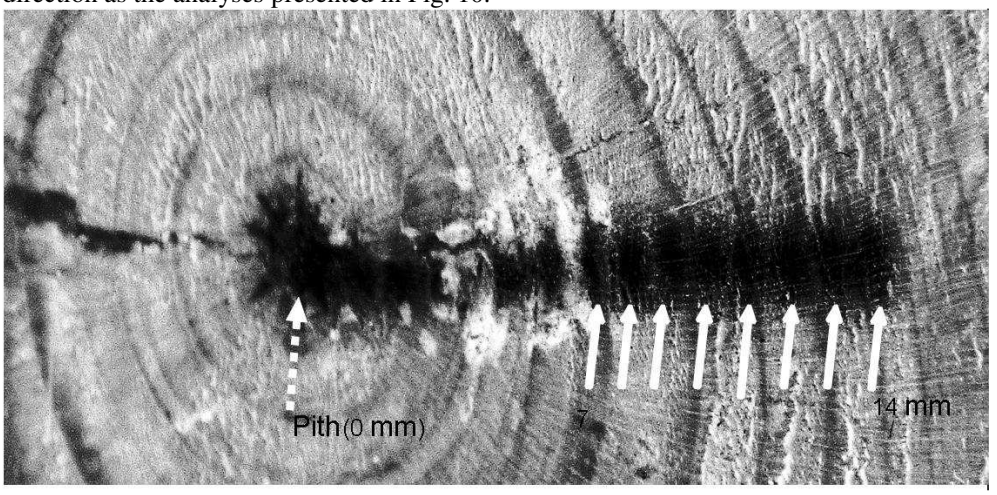

Figure 11. A sample of pine heartwood across which a point scan has been performed in steps of 1 mm, starting from the pith. The pith and the spots at 7-14 mm out from the pith are indicated with arrows.

The concentration profiles obtained for Zn, Ca, Mn and K are shown in Fig. 12. A steep decrease in concentration of all four elements is seen outside a radius including the first 4 spots. For wood at 4-14 mm out from the pith, the variations in elemental concentrations are relatively small. The concentration ranges in this heartwood are for Zn 10.6-15.5, Ca 1530-2120, Mn 164-233 and for K 346-528 mg/kg. The lowest concentrations of Zn, Ca and Mn are obtained for the spot 7 mm out from the pith. Here the proton beam overlaps the clearly broadest latewood ring (Fig. 11). The two following spots (8-9 mm from the pith) both fit into the following, wide earlywood growth – followed by an also relatively wide latewood increment. Especially the concentrations of Zn increase over these three spots, and reach a maximum in the spot 9 mm out from the pith.

Relatively high concentrations of Zn, Ca, Mn as well as K are also seen at the last spot analysed, at 14 mm out from the pith. This spot includes earlywood between two thin latewood increments.

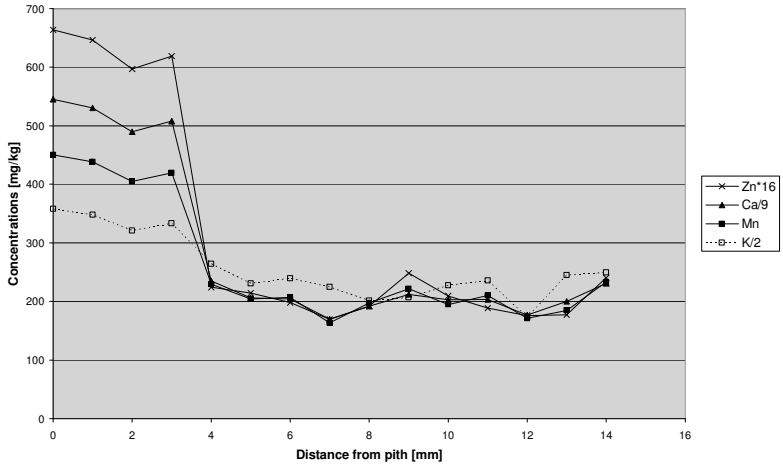

Figure 12. Concentration profiles obtained in the 15 point scan of the pine heartwood sample in Fig. 11. The scaling factors are shown in the insert.

The ion beam technique used gives the concentration of a number of elements within an area of sample surface that is restricted by the diameter of the beam used. As the analyses were performed with a 1 mm diameter beam, correlations between concentrations of elements could be obtained for very restricted amounts of wood tissue (compare Table 1, in section 2.2.1). At spots 4-14 mm out from the pith in Fig. 12, representing alternating early- and latewood of heartwood, the strongest correlation is between Ca and Mn ($r_{Ca\text{-}Mn}$ = 0.946). Clear positive correlations are, however, seen between all divalent cations ($r_{Mn\text{-}Zn}$ = 0.864, $r_{Ca\text{-}Zn}$ = 0.813). Correlations with, the univalent, potassium is much weaker ($r_{K\text{-}Zn}$ = 0.291, $r_{K\text{-}Mn}$ = 0.532 and $r_{K\text{-}Ca}$ = 0.681).

The data from this and the two other scans across innermost pine stem wood are summarized in Table 6. For the sample from the crown part of the pine from Aura, mean values (n=4) are calculated for elements in the wood closest (0-3 mm) to the pith as well as for wood outside this “plateau” of higher elemental concentrations (4-14 mm, Fig. 12). It is seen from Table 6 that the concentrations of zinc are on average 3.1 times higher in the wood closest to the pith, including two annual growth rings, than in the surrounding heartwood. In the same four spots irradiated the concentrations of sulphur could be quantified to 530±30 mg/kg (n=4). In wood more than 3 mm out from the pith concentrations of sulphur varied around a mean value that is close to the detection limit for this element (LOD of approximately 130 mg/kg).

In the sample from Turku (Table 6) the concentrations peaked in the first spot irradiated, and went down half way to “base level” already in the next spot (did not fully fit into the area of the pith). The concentrations obtained for the pith, and the mean values of the concentrations at 2-14 mm from this first spot irradiated, are included in Table 6. The concentrations of sulphur were low, and close to the detection limit, in all 15 spots of the scan across this pine heartwood sample

Table 6. A summary of the concentration data obtained in point scans across the innermost wood of pine wood samples from Aura (compare Figs 11 and 12), Jakobstad (Figs 13 and 14) and Turku. The elemental concentrations are for the centre of the disc showing clearly higher concentrations (exclusively pith in the cases of wood from Jakobstad and Turku), and for the spots outside this radius. The quotient represents the ratio between the pair of concentration values. All concentrations are given in mg/kg of dry wood.

	Aura			Jakobstad			Turku		
element	0-3 mm	4-14 mm	quotient	0-1 mm	2-18 mm	quotient	0 mm	2-14 mm	quotient
Zn	39.5±1.9	12.7±1.6	3.1	44.5	12.5±2.0	3.5	40	14.7±1.2	2.7
Ca	4670±220	1830±180	2.6	3240	1360±150	2.4	4360	1860±260	2.3
Mn	430±20	200±20	2.1	277	124±16	2.2	363	186±17	2.0
K	680±30	454±50	1.5	768	449±47	1.7	851	554±67	1.5
Sr	10.6±0.5	4.9±1.7	2.1	7.8	3.1±1.9	2.5	20.3	8.7±1.5	2.3
S	530±30	220±110		280	230±130		245	130±80	

.

The tree from Jakobstad had been rather fast growing with up to 3-4 mm wide year rings as can be seen in Fig. 13. This enabled separate analyses of earlywood increments. The sample was moved in front of the proton beam with the intention to acquire the first spectrum during irradiation of the centre of the pith (unfortunately the hit was a bit low, compare Fig. 13). Data for the next spectrum was accumulated from a spot 1 mm outwards. After this data acquisition was alternately from two parallel spots, from one single spot and so on, leaving the (adequate) X-pattern seen in Fig. 13.

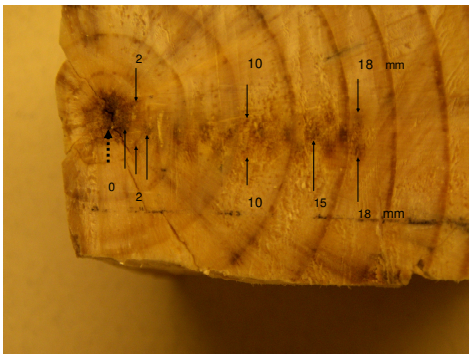

Figure 13. A sample of innermost heartwood of a pine from Jakobstad, analysed to reveal the distribution of elements from the pith and outwards. The arrows indicate the radial distances of spots to the first spot irradiated (the pith).

The concentration profiles obtained for the pine heartwood sample in Fig. 13 are seen in Fig. 14. Unfortunately the spectrum representing wood at 6 mm out from the pith was lost. In Fig. 14 the concentrations of zinc were multiplied, and the concentrations of calcium and potassium divided, by scaling factors to enable better visual comparison of the trends. The scaling factors used were obtained by comparing the mean concentrations of these elements in spots at 2-18 mm from the pith (table 6) with that for manganese. As for the other pine wood samples in Table 6, high concentrations of elements are found in the pith, in this case

represented by the first two (single) spots analysed. However, already outside the pith, at 2 mm, the concentrations drop to levels after which variations are very small, or within the ranges 9.3-13.8 mg/kg for zinc, 1140-1450 mg/kg for calcium, 95-150 mg/kg for manganese and 380-550 mg/kg for potassium.

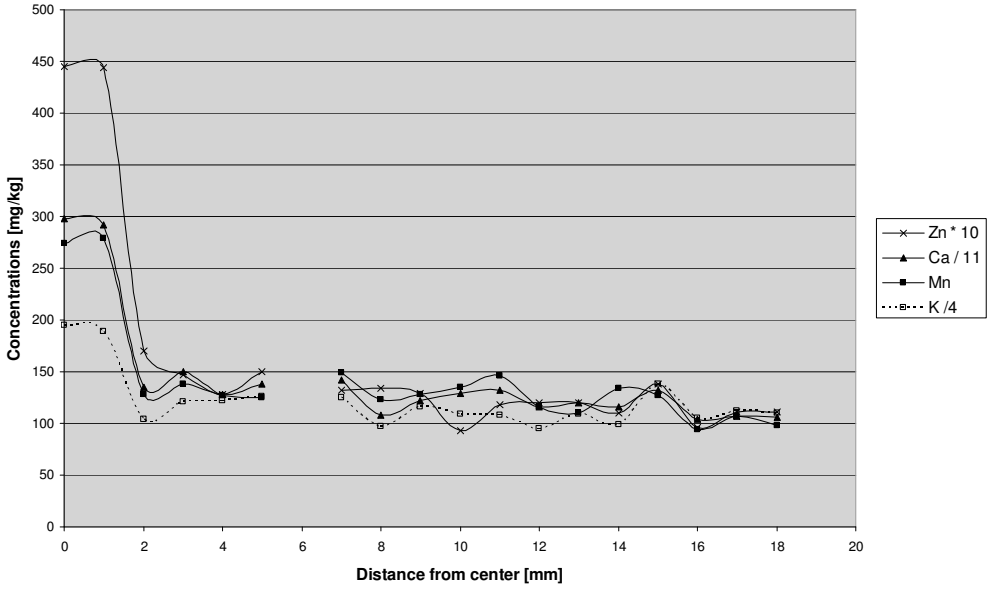

Figure 14. *Radial distributions of elements in the pine stem wood sample shown in Fig. 13. .The scaling factors are shown in the insert.*

Only for manganese some more systematic trend can be seen for the distribution of the element in the innermost heartwood of the pine wood. Local concentration maxima are seen in wood at distances of 7, 11 and 15 mm from the pith, representing the first part of earlywood increments.

3.3.2.2. A scan across heartwood further out from the pith

In **paper I** a scan across pine heartwood from Harjavalta in south-western Finland was performed. The pine studied was felled in 1994 at 6 km from the local copper-nickel smelter that had started its activity about half a century earlier. The disc sampled included 54 growth rings and was scanned outwards starting from the seventh growth ring from the pith. Results of this study are shown in Fig. 15. A decreasing trend outwards is seen for elemental concentrations in the 15 point scan (Fig. 15). The seasonal variations in concentrations were moderate. However, some local maxima can be seen for earlywood in Fig. 15. A clear local minimum is seen for calcium in the widest latewood increment.

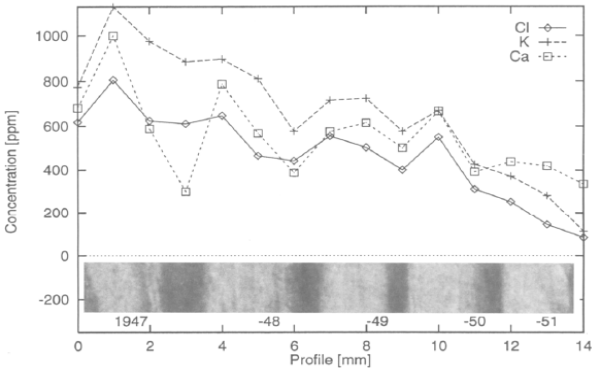

Figure 15. Concentration profiles obtained in a 15 point scan across heartwood of Scots pine from Harjavalta (Fig. 5, **paper I**). A photo of the sequence of annual growth rings (with lighter early wood and darker latewood increments) scanned is included in the figure. Concentrations are in mg/kg (ppm) of dry wood.

3.3.3. Elemental distributions in the innermost heartwood of a medieval pine log sample

The innermost wood of a medieval pine log (Fig. 16) was also analysed. The well preserved log was found during excavations undertaken close to the Aura river in the city of Turku, before the construction of the Åbo Akademi Gripen-building. As the water permeability of heartwood is also known to be very limited, comparison with the "fresh cut" wood samples (Figs 11 and 13) was performed. According to the dendrologist the tree in Fig. 16 was felled during late spring –early summer of 1406. The sample of innermost heartwood analysed (seen in Fig. 16) thus represents wood formed late back in the 14th century.

Figure 16. The cut medieval log, together with the scanned sample of the innermost heartwood.

The log was estimated to have been covered by soil since the middle of the 15th century, or for around 550 years. It was found at a depth of almost 3 meters in a wet and basically oxygen free environment (Pihlman 2009). About half a meter of the log was cut off and brought to the laboratory. The scanned sample in Fig. 16 was prepared from a thin disc from the cut end of this piece of pine log. The concentration profiles obtained in the scan are seen in Fig. 17.

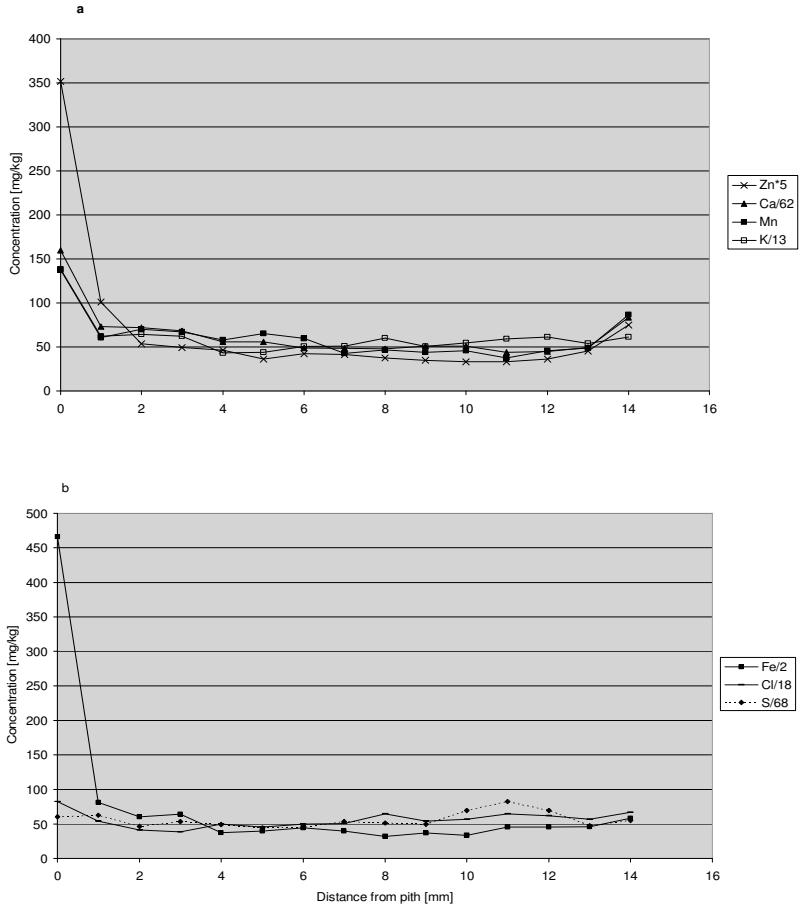

Figure 17. Concentration profiles for: a) Zn, Ca, Mn and K; b) Fe, Cl and S obtained from the radial scan across the sample of medieval pine wood in Fig. 16.

As can be seen in Fig. 17a the elements Zn, Ca, Mn and K all show clear maximum concentrations in the first spot representing the pith. Outside of the pith the concentrations drop radically, and vary very little going outwards in the surrounding heartwood. The concentration data from the scan across the over 600 years old pine heartwood are summarized in Table 7. A comparison with the concentrations in Table 6 shows that:

- Concentrations of S, Cl and Fe are much higher in the pith of the medieval log sample (Table 7). For the samples in Table 6 the concentrations of these elements were around, or below, LODs of 130 mg/kg, 80 mg/kg and 10 mg/kg respectively. The clearly higher concentrations in the medieval sample indicate uptake from the soil water, where anaerobic conditions keep iron in the reduced and more mobile Fe(II) form. The concentrations of the two anionic elements, sulphur and chlorine, were found at almost similar levels across all the spots scanned (Fig. 17b). Concentrations of Zn, Ca and K were about two times higher in the pith of the medieval sample than in the pith of the samples in Table 6. The concentration of Mn was, however, clearly lower.

- The low concentration of manganese and the high concentration of calcium in the pith of the medieval sample are accompanied by equally low and high concentrations in the innermost wood surrounding the pith. As a result, the ratios between the concentrations for these elements in Table 7 are very similar to those obtained for the samples in Table 6. The same pattern is seen for the other alkaline earth ion strontium. The pattern seen for zinc is different. The concentrations of zinc in wood surrounding the pith is actually a bit lower than for the samples presented in Table 6, and the ratio between the concentrations is thus much higher(7.4). The ration is also very high for iron (9.8).

Assuming that the excess of zinc in the pith of the medieval log is from the soil water, it can be concluded that uptake of Zn^{2+} ions into surrounding heartwood has been negligible during this "equilibrium experiment over extended time". The amount of zinc present in the heartwood seems to be only that incorporated during the time of biological activity of this wood tissue. The dead heartwood, on the other hand, seems to have an ability to bind calcium ions. These facts can be related to the different roles of the two elements in the xylem. According to Kozlowski and Pallardy (1997) a main role of calcium is for stabilisation of cell walls, while zinc acts as a metal component of enzymes, e.g., as a cofactor for RNA polymerase influencing protein synthesis in woody plants.

Concentrations of Mn and Zn, as well as K, in the over 600 years old pine heartwood (Table 7) are very similar to the bulk concentrations for stem wood of pine given in Table 5 (from Table 15 in **paper VI**).

Table 7. *Results obtained in the radial point scan across the innermost wood of the medieval log in Fig. 16. The concentration obtained for the pith (0 mm) and the mean and standard deviation of concentrations in spots 1-14 mm out from the pith are given. The last column includes quotients representing the ratios between these concentration values. Concentrations are in mg/kg of dry wood.*

element	0 mm	1-14 mm	Quotient
Zn	70.4	9.5±3.8	7.4
Ca	9900	3510±766	2.8
Mn	137	55.5±13.6	2.5
K	1780	722±91	2.5
Sr	36.5	14.7±5.1	2.5
S	4120	3800±761	1.1
Cl	1480	970±160	1.5
Fe	933	95.2±27.7	9.8

3.3.4. Point scans across annual growth rings in sapwood of spruce and pine

3.3.4.1. Sapwood of spruce

Concentration profiles obtained in a linear point scan across 18 mm of sapwood from a Norway spruce (*Picea abies*) are seen in Fig. 18. The tree was felled in 1994 at 6 km northeast from the copper-nickel smelter at Harjavalta, south-western Finland. The target

sample was prepared from a disc, from the lowest end of the tree, in which 80 tree rings were counted. The 18 spots irradiated represented wood formed during the years 1979-1981. Large seasonal variations in the elemental concentrations were seen for the sapwood scanned. Especially for Fe the range of concentrations was broad, from below the detection limit of 14 mg/kg up to 174 mg/kg. Also for K (200-930 mg/kg), Ca (600-2200 mg/kg), Sr (5-15 mg/kg), Mn (17-58 mg/kg) and Zn (9-25 mg/kg) large variations in elemental concentrations can be seen. The tree rings in the sample analysed in Fig. 18 were up to 6 mm wide, and this enabled analyses of several spots within each annual ring.

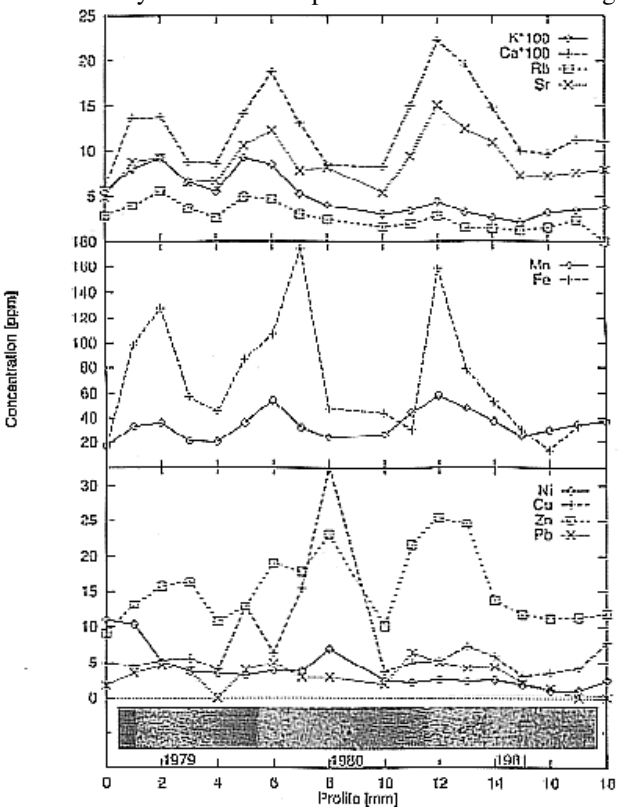

Figure 18. The concentration profiles obtained in a radial scan across sapwood of a spruce tree from Harjavalta, south-western Finland (Fig. 4, **paper I**). Observe that, in this case, the concentrations for elements Ca and K, read from the Y-axis, should be multiplied by a factor 100 to get the concentrations obtained in the PIXE-analysis. Concentrations are in mg/kg of dry wood.

The lowest concentrations of, for example, Ca, Mn and Zn in Fig. 18 are generally seen for spots representing latewood. High concentrations of these elements are seen especially for the earlywood formed at the very beginning of the growth season (early earlywood). An increasing trend towards the bark can be seen for these elements when comparing concentrations in the earlywood of the year rings. Concentrations of zinc are high in all spots within the wide earlywood increment representing the year 1980. The growth was good during this year, and the latewood increment is also wide.

The elemental concentrations are generally lower in spots representing latewood, an example is the spot at 10 mm in Fig. 18. Increases in concentrations of, for example, Ca, Sr and Zn can, however, be seen going outwards in latewood (e.g., at 10-11 mm), towards earlywood of

the following growth season. This implies radial translocation of ions from sap in earlywood, to binding sites in the denser latewood. In this connection it could be mentioned that analyses of the wood inside a Cr- and Cu-impregnated board showed that these two elements were enriched in latewood, while the Ca concentrations remained higher in earlywood (supporting paper 8). This observation could be related to the fixation process being driven by an oxidative reaction of chromate, Cr(VI) → Cr(III), with wood (Bull 2001). According to Bull (2001) large numbers of carboxylate groups should be generated in this reaction by oxidation of lignin and carbohydrate fractions.

Distinct concentration maxima for iron can also be seen in earlywood in Fig. 18. Copper concentrations are mainly below the limit of quantification (ca. 4 mg/kg). In some spots the concentrations are, however, clearly higher. The two highest concentrations of copper are found within earlywood representing the growth during 1980, peaking in the late earlywood. The concentration found in the latter spot is 30 times higher than concentrations obtained in bulk analyses of spruce stem wood (**paper VI**). Berglund et al. (1999) found "hot spots" of Fe and Cu in spruce sapwood. These local high concentrations were explained as a part of the metals being arranged in inorganic precipitates instead of being attached to the "hemi cellulose/lignin matrix". In Fig. 18 the very distinct concentration maximum for Cu (and also Fe) occurs later in the wide earlywood increment of the year 1980 than those for Ca or Mn. This could be taken as support for an assumption that the metal ion is precipitated with some component dissolved in the sap water having passed through this wide earlywood increment.

3.3.4.2. Sapwood of pine

A distinct peak for copper can also be seen in the concentration profile in Fig. 19, obtained from a scan across sapwood of pine from the same location as the spruce in Fig. 18. The high concentration of copper is found in a spot representing earlywood. The concentration of zinc was also high in this same spot. Zinc concentrations showed clear seasonal variations and a general increasing trend towards the bark in the pine sapwood sample.

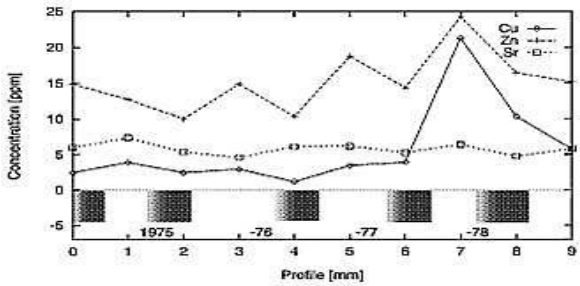

Figure 19. Concentration profiles obtained from a 10 point scan across pine stem wood (sapwood) of a tree from Harjavalta (Fig. 3, **paper III**). All concentrations are given in mg/kg of dry wood (ppm).

3.3.5. Comments to results obtained in the radial analyses of stem wood

Published data on the radial distribution of elements in stem wood are relatively scarce and do not always agree. In the rather few reports found considering elemental distribution in and between the annual growth rings, it is also not always mentioned if heartwood or sapwood is analysed. Reports on the determination of elemental concentrations in the pith, or the pith region, seem to be even non-existing.

In the reports found where elemental concentrations in earlywood and latewood have been studied, the concentrations in earlywood are generally higher. Tokareva et al. (2007) found higher concentrations of Ca, Mg, Na and K in earlywood than in latewood of spruce (Picea abies) sapwood. In heartwood, however, this trend was not seen for Ca and K. Lövestam et al. (1990a) also reported higher concentrations of elements, including Ca, Fe, Cu and Zn, in the earlywood of spruce. The same authors also stated that the concentration patterns for potassium and chlorine "do not show a pronounced ring structure". Kuczumov et al. (1996) also found these univalent ions to be very irregularly distributed in pine wood, but reported that the concentrations of Ca, Mn and Fe followed the density patter, i.e. concentrations were higher in the less dense earlywood than in latewood. Kuczumov et al. (1996) also noted that the maximum concentration of calcium in the earlywood was found closest to the dense latewood of the preceding year.

The width of an annual growth ring, formed in a tree, is substantially reduced by drought (Kozlowski and Pallardy 1997). Essentially all water absorbed by roots moves upwards through the stem and branches to the evaporating surfaces of the foliage (Kozlowski and Pallardy 1997). This flow is via the sapwood, and mainly an outer section of this younger xylem. The earlywood of the annual growth rings in the sapwood is the major path for the flow, as latewood is much more resistant to water transport (Kozlowski and Pallardy 1997). Large amounts of aqueous solution will thus pass through this earlywood during a growth season, especially if precipitation is large. Elements/ions can thus be bound to functional groups, precipitated or otherwise incorporated into the wood-structure, from this upward flow of water from the roots. This can be seen as seasonal variations of elemental distributions in for example Figs 18 and 19 of this thesis, with higher concentrations in the earlywood of the sapwood. Translocation of elements would explain the higher concentrations seen outwards in latewood increments (Fig. 18), as well as the small seasonal variations seen on the mm-scale in heartwood (Figs 12, 14, 15 and, especially, Fig. 17)

Outwards decreasing trends for concentrations of alkaline earth metals, found in coniferous stem wood, have been ascribed to decreasing cation binding capacity of the wood from pith to bark (Meerts 2002). A decreasing trend from pith to bark was seen for calcium and manganese in the analyses presented in Fig. 10. Concentrations of zinc were very evenly distributed across the heartwood. The lowest concentrations of zinc were found in the inner sapwood closest to the heartwood, after which an increasing trend was seen towards the bark (Fig. 10). The transformation into sapwood is gradual (Pallardy and Kozlowski 1997). The concentration profile for zinc (fig. 10) could thus be interpreted as an emigration of this element from older sapwood, in transformation into heartwood, to outer, biologically more active regions of the stem. This would mean clever "recycling", which fits the role ascribed to zinc in woody plants as being a cofactor for RNA polymerase influencing protein synthesis (Kozlowski and Pallardy 1997), as the stem radius increases with each annual growth ring formed.

In Fig. 18 the concentrations of zinc were shown to be the highest in earlywood, i.e. the wood representing the start of a growth season. The importance of zinc in the growth process of an individual tree is also indicated by the relatively higher concentrations of this element in the pith, as shown for pine stem wood in Table 6. The pith in a disc of stem wood is the tissue formed during the first year of radial growth, and it represented the growing point of the tree when the tree was of the height at which the disc was sampled from the tree felled. An around 3 times higher concentration of zinc was found in the pith, compared to the surrounding wood, for all the pine samples studied (table 6 on page 33). Concentrations of the plant essential elements Ca and Mn were also clearly higher in the pith of the samples. At crown level in a pine tree this "pith like" feature was extended over a radius including the first two annual growth rings (Figs 11 and 12).

3.4. Representative sampling of stem wood – analyses of birch

The sampling is essential when concentrations representative of, for example, the bulk of a disc of stem wood are desired. With the results from this analysis, questions that can be asked are: how representative are these results for the stem as a whole, or, for stem wood of this tree species in general?

The results presented in Table 8 are from analyses of birch wood sampled in different ways. All bark was removed from the samples, and the wood was dry ashed at 550 ˚C. The ashes obtained were homogenised by shaking, and pellets for PIXE analyses were prepared as described in chapter 2. None of the sampled sites were known to have been exposed to any pollution of the soil.

The four categories of samples (a-d in Table 8) were:

a) Samples taken from the same disc of a tree. A disc of birch stem wood was cut into eight (n=8) equally large 45˚ sectors. The disc was from the lower end of the stem of a birch from Kållby, Ostrobothnia. The whole sectors of wood were dry ashed for PIXE analyses (**paper VI**).
b) Discs cut from six different heights (n=6) of the same tree. Discs were cut from the base and from heights of 6, 8, 10, 12 and 14 m in the same tree. The whole discs of wood were dry ashed for PIXE analysis.
c) Samples from seven (n=7) different trees growing within a limited area of 0.02 ha at Nykarleby, Ostrobothnia (**paper IV**). A disc was cut from the lower end of each tree. From each disc a sector of wood was removed and dry ashed for PIXE analysis.
d) Samples from five different trees (n=5) growing within an area of 1 ha on the island of Nagu in the Turku Archipelago (**paper VI**). A disc of stem wood was cut from the lower end of each tree. From each disc a sector of wood was removed and dry ashed for PIXE analysis.

Although the number of samples in each category is different (n= 5-8), it can be concluded from the relative standard deviations (RSDs) in Table 8 that the greatest differences in elemental concentrations generally are between individual trees. This although the individual trees of respective groups c) and d) had grown within very restricted areas, and thus under similar climatic conditions. Apparently, the root systems of individual trees find quite different amounts of the plant available ions, even when the trees are growing close together.

Table 8. Elemental concentrations obtained in analyses of: a) the eight 45 ˚ sectors of the same disc of a birch from Kållby, b) whole discs from 6 different heights in a birch from Vexala, Nykarleby, c) single sectors of discs from 7 different birch trees growing within 0.02 ha in Nykarleby (from **paper IV**), and d) single sectors of discs from 5 different birch trees from the Nagu island in the Turku archipelago. All concentrations are in mg/kg of dry wood.

	a) 8 sectors of a disc		b) 6 different hights		c) 7 different trees		d) 5 different trees	
	mean	RSD [%]	mean	RSD [%]	mean	RSD [%]	mean	RSD [%]
ash[%]	0.31	4.3	0.35	11	0.32	21	0.389	26
P	54.2	18	87.6	39	144	20	142	33
S	30.4	18	46.4	31	125	23	189	49
K	469	13	458	13	619	44	840	18
Ca	254	18	425	12	847	40	1170	70
Mn	22.2	17	63.6	10	121	45	132	109
Fe	2.15	13	1.16	32	3.3	22	17.1	74
Cu	0.964	4.8	0.74	16	1.16	13	1.03	35
Zn	36.2	13	15.7	17	35	21	48.4	37
Rb	2.59	7.0	2.14	12	3.9	29	4.18	19
Sr	5.23	9.1	3.79	11	5.7	18	5.48	32

For 8 out of the 11 elements quantified in table 8, the largest variations are seen for samples from the trees at Nagu, and variations are the largest for Ca, Mn and Fe. Of these elements, manganese and iron can occur at more than one oxidation state.

Martin et al. (2006) related high variations in metal contents between trees at the same site to the complex nature of the uptake by trees, and different micro-environments experienced by the individual trees. The metal content of forest soil varies over small distances, and the metal being bioavailable, or in a form that can be made bioavailable, depends on small-scale (near tree) variations in soil pH, pE (redox conditions), mineral and organic content, fungi, micro topology etc. (Martin et al. 2006).

For the eight sectors of the same disc of a tree, a) in table 8, the differences in both ash and elemental content are found to be small. The variations for samples taken from different heights in the birch b) are also relatively small compared to those between individual trees. Only for phosphor a larger variation is seen sampling from different heights in a tree. Comparing the results for these two birches, a) and b) in Table 8, from sites about 40 km apart in Ostrobothnia, it is seen that only a few of the ranges set by the standard deviations for the elemental concentrations overlap.

The relative concentrations of elements at different heights in birch b) in Table 8 are shown in Fig. 20. The concentrations at the different heights were normalized so that the mean concentration for respective element (from Table 8) is represented by the value 100 on the Y-axis. The diameter of the tree at the base was around 30 cm. At the height of 14 m the stem had a diameter similar to that of the main branches, or less than 5 cm. At least the last 2 meters of stem in Fig. 20 would thus have been left as residue in normal harvesting of birch log.

The greatest variations with height are seen for Fe, P and S. The variations in the concentrations of Fe are irregular, and greater than for any other metal quantified (Fig. 20). A steep increase is seen towards the top of the tree. For sulphur and phosphor, both elements that are present as anions in aqueous solutions, clearly increasing concentrations with height can bee seen, especially in the upmost 2 meters of thin stem wood.

Essentially all water absorbed by roots moves upwards through the stem and branches to the evaporating surfaces of the foliage (Kozlowski and Pallardy 1997, Martin et al. 2006). Transpiration is the driving force that maintains the transportation of dissolved elements up through the tree, and the transpiration rate for birch is high due to the large leaf area (Kozlowski and Pallardy 1997). The increase in concentrations of the anionic elements up the birch, demonstrates that the tree stem is principally a cation binding column. The similar profiles seen for iron and phosphor in Fig. 20 could indicate possible precipitation of iron as the phosphate, especially in the crown part of the tree.

The elemental concentrations obtained for the sample from the low end of the stem are generally relatively close to the mean value (close to the value 100 in Fig. 20). Especially when one considers that the lower end of the stem is thicker, and thus represents a larger amount of the total biomass, the conclusion can be drawn that cutting the disc from the lower end of the tree, gives samples with elemental concentrations well representative of the bulk of the stem.

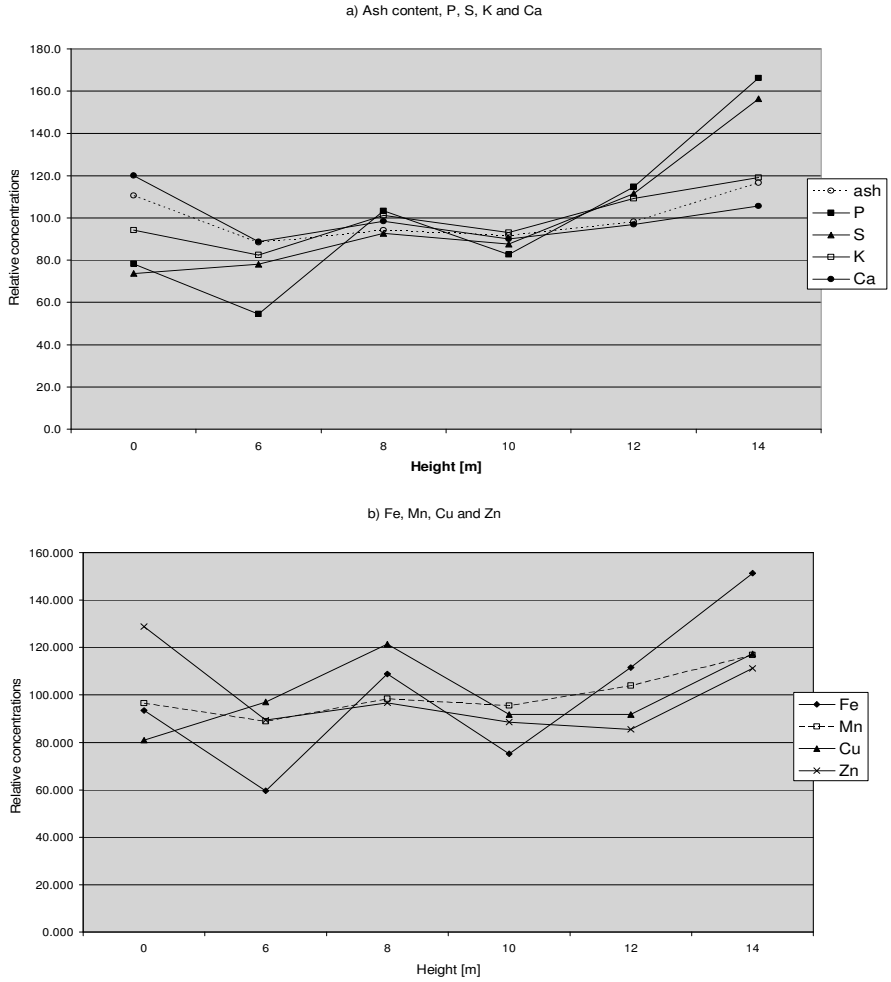

Figure 20. Relative concentrations of a) main mineral elements and b) some trace metals, at different heights in the stem of a birch from Nykarleby.

3.5. Elemental distributions in some pine bark samples

The first step in the pulp manufacturing process is the debarking of the logs used as raw material. The bark removed is mostly burned for production of heat and energy. Ashes from combustion of the biofuel can be reused, e.g., in the cement and brick industry, and also have a great potential to be used as fertilizer.

Pine tree barks have shown to be good sorbents of airborne pollutants, including heavy metals (Schulz et al. 1999). Scots pine (*Pinus sylvestris L.)* is abundantly available in the northern coniferous forests and its inert, porous and large surface bark has been used in the monitoring of atmospheric metal pollution (Lippo et al. 1995, Poikolainen 1997). Bark is exposed to air pollution either directly from the atmosphere or from stemflow, which also brings down pollutants deposited on higher parts of the tree. (Schulz et al. 1999, Poikolainen 1997). According to Schulz et al. (1999) the external bark sheet of a pine is rejected after approximately 2 years. The pine bark used in the monitoring of atmospheric pollution has often been sampled by removing ca 2-3 mm of the bark surface at breast height (Lippo et al. 1995, Poikolainen 1997, Schulz et al. 1999, Pöykiö et al 2005).

The concentration profiles from point scans across pine bark samples from two different sites are shown in Figs 21 and 22. The scans were performed in steps of 1 mm from inner bark to the outer surface of the bark. The scan in Fig. 21 was across 22 mm thick bark of a pine from the Turku archipelago (Nagu).

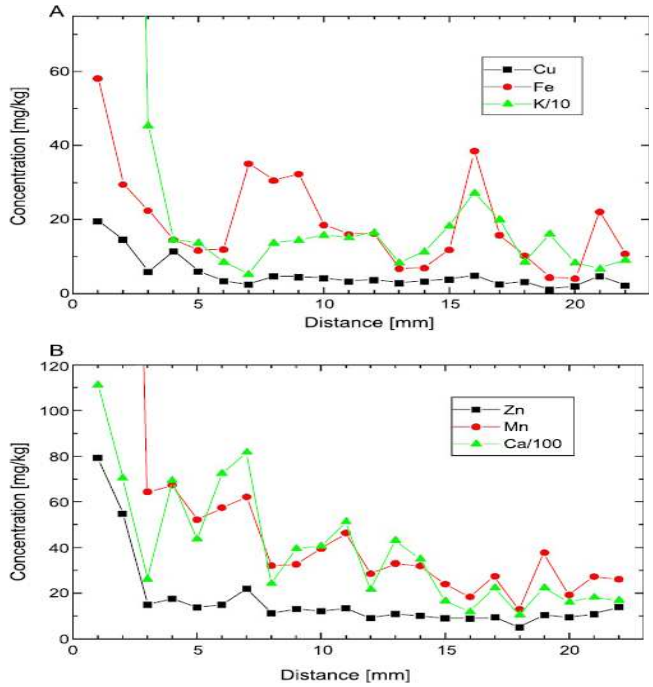

Figure 21. Elemental concentration profiles obtained in a point scan across a pine bark sample from the island of Nagu, south-western Finland. The first 2 spots of the 22 point scan represent inner bark. (Fig. 3, **paper V**).

This 22 point scan from the inner bark to the outermost cork bark layer revealed large variations in the elemental concentrations (Fig. 21). The sample represents pine bark not exposed to atmospheric pollution from any identified source of emission. Clearly higher concentrations of potassium and manganese are seen in the two first spots, representing the inner bark. The concentrations of zinc were also 3-4 times higher in these two spots than in the rest of the bark scanned. Concentrations of Fe varied strongly through the whole of the bark. The same is valid for calcium and manganese. The concentrations of these two elements show a similar pattern in the outer bark. Calcium is known to occur mainly as the oxalate in bark (Kozlowski and Pallardy 1997). The similar concentration profiles for these two elements in Fig. 21 suggest co-precipitation of manganese.

The concentration profiles in Fig. 22 were obtained from a scan across bark from a 25 year old pine tree that grew at a distance of 600 m from a metal plant (supporting paper 11). The profiles show that the highest enrichment of all the three heavy metals is in the mid section of the outer bark. Less than 1 mm of the 8 mm thick bark sample from this polluted site was inner bark.

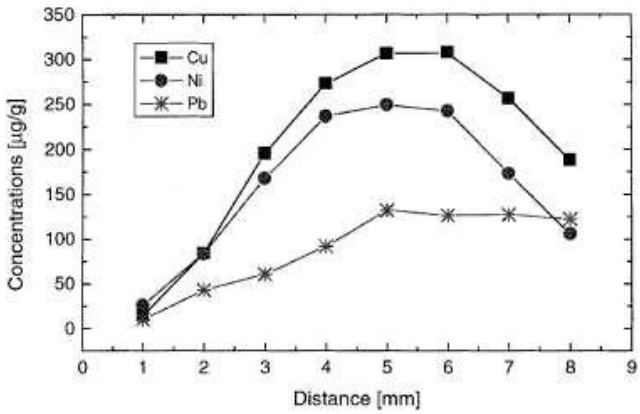

Figure 22. Elemental concentration profiles for a pine bark sample from a site at 600 m from the zinc plant in Yxpihlaja, Kokkola (supporting paper 11). The point scan is started from the inner bark (first spot, left)

Results from analyses of the inner and the outer bark of a pine bark sample from Turku are presented in Table 9. To obtain results representative of a larger amount of the inner and the outer bark respectively, the two bark layers were separated and dry ashed at 550 °C. The two ashes were homogenised by shaking and analysed with PIXE.

It can be seen that the concentrations of most elements are about the same in the inner and the outer bark, and the ratio between these concentrations have values close to 1 (Table 9). The concentration of manganese was somewhat higher in the inner bark, but clearly the largest differences were seen for potassium and phosphorus. In the sample studied the concentrations of these two elements were an order higher in the inner than in the outer bark. The bulk concentration of calcium in the inner bark was lower than the bulk concentration of calcium in outer bark of this specific sample. The concentrations of elements were generally in line with the concentrations obtained from analyses of a larger number of samples of whole bark of pine (Table 15, **paper VI**), and can on this basis be considered to represent normal background concentrations.

Table 9. Ash content (%) and elemental concentrations (mg/kg) in inner and outer bark of a pine bark sample from Turku (**paper VI**). Ratios between the concentrations in inner and outer bark are also included. The mean values in the table are concentrations obtained from analyses of a larger amount of samples of whole bark of pine (n= 21, table 15 in **paper VI**). All concentrations are given as mg/kg of dry bark.

Element	inner	outer	inner/outer	Mean	±RSD [%]
Ash [%]	2.33	0.929	2.5	2.03	58
P	408	23.8	17	482	89
S	258	81.9	3.2	834	69
K	2350	191	12	2147	86
Ca	2750	4270	0.64	7938	63
Mn	252	94.3	2.7	216	116
Fe	74.6	84.2	0.89	102	101
Ni	0.92	0.51	1.8	1.2	79
Cu	3.37	3.19	1.1	3.2	30
Zn	33.8	19.2	1.8	32	78

Lövestam et al. (1990b) performed a radial scan across the outermost wood and the bark of a Scots pine, using PIXE, presenting concentration profiles for Cl, K, Cu, Ca, Mn and Zn. All profiles except that for (the anionic) chlorine showed a clear increase in concentrations passing from wood to bark. Distributions of the elements were relatively uniform within the bark. For Cl and Cu higher concentrations were seen for the outermost part of the bark (no information concerning the sampling site was given). Raunemaa and co workers (1987) performed a scan across pine bark from a non polluted site (Salpausselkä). They found an increasing trend outwards for Ca, Mn and Fe. For elements like Cl, S, K, Ni, Cu and Zn no trends were seen.

The studies mentioned above (Raunemaa et al. 1987, Lövestam et al. 1990b) and the concentration profiles presented in Figs 21 and 22 in this thesis, suggest that the sampling, or more specifically the thickness of the bark layer taken for analysis, can be critical and strongly affect the result of a study aiming at monitoring atmospheric pollution. The (bulk) analyses of pine, spruce as well as birch bark in the present work are for the whole bark, i.e. all layers of the bark are included. The bark samples were from the lower end of stems. In the case of especially pine, this means that the cork bark layer is thicker, with more cracks. This should mean that sorption of inorganic pollution from a downwards stem flow is greater.

3.6. Bulk analyses of stem wood and bark

In the following section, results obtained from bulk analyses of stem bark and wood are discussed. Sectors of wood to be analysed were sampled from discs to take variations in radial distributions of the elements into consideration. Whole bark was sampled consistently due to the large variations in the distribution of elements observed within bark. The elemental concentrations reported are thus also representative for the bark obtained from debarking of logs for pulping.

Samples were dry ashed at 550 °C and the ashes shaken to eliminate the effects of the inhomogeneities shown already at mm-scale. The enrichment obtained through dry ashing also enabled quantification of the concentrations of some metals present at trace element levels. For example, copper and iron could be quantified in all wood and bark samples analysed.

Variations in elemental contents of stemwood and stembark with harvest season were shown to be moderate by Werkelin (2008). Most samples analysed in this thesis were taken in connection with logging, normally during winter. The trees sampled were, thus, mature and healthy individuals, growing in forests. The fact that the trees were growing in a forest also means that the soil had a full vegetation cover. This cover effectively prevents the dispersion of soil particles or dust that could easily be incorporated into a cork bark layer on, e.g., a Scots pine

Pieces of log were cut off from the lower end of straight and symmetric trees, above the stump. The knot-free disc, from which material was taken for sample preparation, was cut from the thinner end of the piece of log. The wood and bark analysed thus was from about 0.5-1 m above the ground level in the forest.

3.6.1. Bulk analyses of stem wood and bark of pine and spruce trees exposed to atmospheric pollution

3.6.1.1. Pine stem wood and bark

In **paper V** sectors of pine wood, as well as the bark outside these sectors, were analysed. The samples were from three different areas: the island of Nagu (Turku archipelago), Ostrobothnia (mid-western Finland) and Harjavalta (south-western Finland). Discs of 3 pines from Nagu and 8 pines from 4 different sites in Ostrobothnia were included in the study. The 3 discs of pine stem wood from Harjavalta were from trees growing 6 km northeast of the local copper-nickel smelter. Until 1989 the smelter was neighboured by a fertilizer factory, which was estimated to emit 1 ton of phosphorus annually (Derome and Nieminen 1998)

From the results summarized in Table 10, it can be seen that the elemental concentrations in bark vary strongly for the bark samples from the different areas. The ash contents and elemental concentrations of pine barks from Ostrobothnia are generally higher than for the bark samples from, for example, the Turku archipelago. (Nagu). A pollution factor (Pöykiö et al. 2005), also named bioindication index (Schulz et al. 1999), is often determined as the ratio between metal concentrations found in bark samples from an area studied and those in

samples from a selected background site, assumed to be unpolluted.. Comparing the higher concentrations of manganese and iron in pine barks samples from Ostrobothnia to those obtained for samples from Nagu, pollution factors of around 14 and 5, respectively, are obtained.

Table 10. Ash contents (%) and elemental concentrations in the bark and the wood of pine stems (**paper V**). The three groups of pine trees were from an area of 1 ha on the island of Nagu, from different sites in Ostrobothnia (mid-western Finland), and from a spot at 6 km from the copper-nickel smelter at Harjavalta. a = the mean of the ratios between the concentration in the bark and the concentration in the underlying wood of the discs of pine stem wood. b) = the same ratio for the concentrations in the corresponding ashes. All elemental concentrations are in mg/kg of dry bark and wood respectively.

	Nagu				Ostrobotnia				Harjavalta			
Element	bark	wood	a	b	bark	wood	a	b	bark	wood	a	b
Ash [%]	1.31	0.27	4.9		3.04	0.33	9.2		0.92	0.23	4.0	
P	382	112	3.4	0.7	746	58	13	1.4	164	64	2.6	0.6
S	345	111	3.1	0.6	853	62	14	1.5	329	84	3.9	1.0
K	1610	620	2.6	0.5	3170	596	5.3	0.6	651	448	1.5	0.4
Ca	7230	689	10	2.1	12700	789	16	1.7	4460	487	9.2	2.3
Mn	31	32	1.0	0.2	432	83	5.2	0.6	71	58	1.2	0.3
Fe	33	9.7	3.4	0.7	162	12.9	13	1.3	147	1.9	77	**20**
Ni	0.60	0.21	2.9	0.6	1.71	0.13	13	1.4	18	0.34	53	**14**
Cu	3.5	0.59	5.9	1.2	3.4	0.86	4.0	0.4	89	0.96	93	**23**
Zn	15.0	11.7	1.3	0.3	45	5.6	8.0	0.9	43.3	7.8	5.6	1.4
Rb	10.9	3.8	2.9	0.6	19.5	2.4	8.1	0.9	1.6	1.0	1.6	0.4
Sr	12.3	2.8	4.4	0.9	22.0	2.9	7.6	0.8	8.9	1.4	6.4	1.6
Pb	1.0	0.10	10	2.1					9.1	0.08	114	28

The elemental content of a pine bark sheet can be related to the availability of different nutrients and elements at the time of its formation (Raunemaa et al. 1987). The availability of the elements from the soil, as well as local climate conditions, will thus affect the elemental composition of the bark. An attempt to take these facts into consideration in the monitoring of atmospheric pollution, using pine bark as an indicator, was done in **paper V** by:
a) comparing the concentration of an element in the bark to that in the underlying wood, and by
b) doing this comparison using the concentrations in the dry ashed materials.

The ratio between the concentration in bark ash and the concentration in wood ash was close to 1 for most elements (table 10). Or, to put it simple, dry-ashing of the bark and the underlying wood generated ashes, with basically similar concentrations of the elements. Ratios were generally the highest, or around 2, for calcium at all sites sampled. The exceptions were for some metals in samples from Harjavalta. The concentrations of nickel, iron, copper and lead were found to be 14 to 28 times higher in bark ash than in wood ash of pine from this site. According to Kiikkilä (2003), the total load of metals to the environment from Cu-Ni smelter at Harjavalta was the highest in 1987, with annual emissions of: 140 tons of copper, 96 tons of nickel, 162 tons of zinc and 94 tons of lead. Since then, technical modifications at the smelter have decreased the emissions considerably. In the year 1994 (the year when the pines at Harjavalta were sampled) the annual emissions had dropped to 40 tons

(Cu), 6 tons (Ni), 6 tons (Zn) and 3 tons (Pb) respectively. The high ratios between elemental concentrations in bark ash and wood ash of the Harjavalta samples (Table 10), verify that the high concentrations of the elements in bark are almost exclusively from the Cu-Ni-plant, still at 6 km distance from the point source of emission. No indication of atmospheric pollution by zinc was obtained at this distance from the point source.

As pointed out earlier, the concentrations of manganese were clearly higher in the pine bark samples from the region of Ostrobothnia (Table 10) than in the pine bark samples from, e.g., the Turku archipelago (Nagu). However, the ratio between the concentration in dry ashed bark and dry ashed wood had a value close to 1 also for this element (0.6, Table 10). This example illustrates how an elevated concentration of an inorganic element in a bark sample, comparing to concentrations in bark samples from a selected background site, could be explained by:

1. A higher bioavailability of the element from the soil. In the above case the concentrations of Mn are also the highest in the stem wood of pine trees from Ostrobothnia (Table 10)
2. A generally more efficient transport of the inorganic element in sap water to the stem surface and the bark forming region. The stembark/stemwood ratios for ash contents are clearly higher (around 9) for the pine trees from Ostrobothnia in table 10.

3.6.1.2. Spruce stem wood and bark

Results from analyses of bark and wood of spruce trees are presented in Table 11. Pieces of logs were delivered from Harjavalta (8 pieces), Nagu (7) and Ostrobothnia (12). In some cases only the wood of the disc of spruce log was analysed.

The samples of bark and wood from Nagu were from 7 trees, growing within an area of 1 ha. The samples from Harjavalta were from trees that had grown at distances of 2-6 km from the copper-nickel smelter. The Ostrobothnian samples (**paper IV**) were from four different sites: Kronoby, Piippola, Pyhäjärvi and Vimpeli.

Comparing the results for wood from the different areas it can be seen that the elemental concentrations are generally of the same level. Variations in elemental concentrations are equally large for the samples from Nagu, where the trees sampled were growing within an area of 1 ha, as for the samples from the two other areas. The concentrations of phosphorus are low in many of the wood samples from Harjavalta (Table 11a), and could be quantified in only 5 out of the 8 samples analysed. The potassium concentrations are generally higher in the spruce wood samples from Harjavalta, but the variations between individual trees are very large.

Copper could be quantified in all bark and wood samples analysed. Concentrations of copper were found to be somewhat higher in spruce wood from Harjavalta. The mean concentration was, however, within the ranges given by the standard deviations for copper in spruce wood from the other areas. Nickel was found at quantifiable levels in all the spruce wood samples from Harjavalta, and the concentrations were also somewhat higher than those quantified in some of the wood samples from the other areas.

Table 11. Ash contents and elemental concentrations in **a)** wood, and **b**) bark of spruces felled at 2-6 km from the copper-nickel smelter at Harjavalta, as well as of spruces from Nagu and from the region of Ostrobothnia. In **c)** the ratios between concentrations in bark and wood are calculated both for the biological and the dry ashed materials. All elemental concentrations are in mg/kg of dry wood or bark.

a) wood	**Harjavalta**			**Nagu**			**Ostrobotnia**		
	Average	RSD[%]	n	Average	RSD[%]	n	Average	RSD[%]	n
Ash [%]	0.536	57.0	8	0.496	47	7	0.343	42	12
P	30.3	50.3	5	130	110	6	95.5	47	11
S	84.5	30.8	6	127	68	7	96.2	41	9
K	1820	94.5	8	1380	56	7	780	29	12
Ca	994	31.8	8	1290	29	7	879	54	12
Mn	76.3	43.2	7	62.9	34	7	97.9	39	12
Fe	4.10	40.7	8	22.2	75	7	5.57	105	12
Ni	0.52	84.4	8	0.39	96	4	0.28	79	6
Cu	1.22	36.1	8	1.00	40	7	0.81	19	12
Zn	14.9	53.3	8	11.3	31	7	7.36	31	12
Pb	0.28	42.3	8	0.55	44	7	0.17	50	3
Rb	4.52	40.1	8	6.3	80	7	3.33	51	12
Sr	5.81	22.0	8	7.7	39	7	6.22	44	12
b) bark	**Harjavalta**			**Nagu**			**Ostrobotnia**		
	Average	RSD[%]	n	Average	RSD[%]	n	Average	RSD[%]	n
Ash [%]	2.14	20	6	3.42	28	7	3.02	78	6
P	531	41	5	1000	61	5	1070	30	6
S	754	22	6	948	38	7	1110	23	6
K	2280	51	6	6430	61	7	5200	26	6
Ca	9530	32	6	16300	29	7	17600	22	6
Mn	221	58	6	249	48	7	971	46	6
Fe	251	85	6	53.4	80	7	104	38	6
Ni	23.7	29	6	2.21	22	2	2.88	58	6
Cu	96.4	79	6	4.34	42	7	5.16	16	6
Zn	107.0	28	6	91.8	34	7	152	38	6
Pb	17.7	133	6	3.16	35	3	1.35	7	3
Rb	8.26	71	6	29.0	77	7	29	37	6
Sr	21.8	36	6	44.2	36	7	60.6	30	6

c) quotients	**Harjavalta**		**Nagu**		**Ostrobotnia**	
	bark / wood	bark ash / wood ash	bark / wood	bark ash / wood ash	bark / wood	bark ash / wood ash
Ash [%]	4.0		6.9		8.8	
P	18	4.4	7.7	1.1	11	1.3
S	**8.9**	2.2	7.5	1.1	12	1.3
K	1.3	0.31	4.7	0.68	6.7	0.8
Ca	**9.6**	**2.4**	**13**	**1.8**	**20**	**2.3**
Mn	2.9	0.73	4.0	0.57	9.9	1.1
Fe	**61**	**15**	2.4	0.35	19	2.1
Ni	**46**	**11**	5.7	0.82	10	1.2
Cu	**79**	**20**	4.4	0.63	6.4	0.72
Zn	7.2	1.8	8.1	1.2	**21**	2.3
Pb	**64**	**16**	5.7	0.83	8.0	0.91
Rb	1.8	0.46	4.6	0.67	8.7	0.99
Sr	3.7	0.94	5.7	0.83	9.7	1.1

The enrichment of inorganic elements in bark is quite different for the three areas. As seen from the bark/wood-ratios in Table 11c, ash contents are from 4 (Harjavalta) to 9 times (Ostrobothnia) higher in the bark than in the stem wood of spruces. Similar regional differences were also earlier seen for pine trees in Table 10, the enrichment from wood to bark was the strongest at Ostrobothnia.

As for pine, the largest enrichment from wood to bark is seen for the element calcium also in the case of spruce. The concentrations of Ca were 1.8 (Nagu) to 2.4 (Harjavalta) times higher in bark ash than in wood ash of spruce (Table 11c).

Comparing spruce bark samples from different regions in Table 11b it can be seen that the clearly highest concentrations of manganese are seen for the samples from Ostrobothnia – which was also the case for pine bark (Table 10). Also these high concentrations of manganese are explained by a large uptake via the roots and a strong, general enrichment of inorganic elements from wood to bark. By dividing the concentration of the element in bark ash, with that in wood ash, a quotient of 1.1 is obtained for the spruces from Ostrobothnia (Table 11c).

From Table 11c it is also seen that for samples from Harjavalta, the ashes of spruce bark contained on average 11-20 times higher concentrations of Ni, Fe, Pb and Cu than the ashes of the wood. The high concentrations of these metals in the bark samples are thus shown to be almost exclusively from atmospheric deposition on the tree.

3.6.1.3. Analysing bark and wood for environmental monitoring purposes

The contents of inorganic elements in a stem of a tree are almost completely from ions taken up in the tree via the root system (Kozlowski and Pallardy 1997, Martin et al. 2006, Watmough and Hutchinson 2003, Watmough et al. 1999)). Some mineral elements absorbed by leaves and bark have been shown to reach the phloem of the tree (Kozlowski and Pallardy 1997). Watmough et al. (1999) studied uptake of zinc and lead via foliage and found it unlikely that this could be a major pathway of metal accumulation in xylem. The studies on uptake through tree bark by Watmough and Hutchinson (2003) showed that lead and cadmium could enter wood through bark under conditions found in heavy pollution areas, but concluded that: “this route of uptake is only of minor importance compared with uptake of Pb and Cd from soil”.

As earlier mentioned, transpiration from the foliage is the driving force that maintains further transport of the inorganic elements from the root up the stem (Kozlowski and Pallardy 1997). This means that duration of sun light, humidity, mean temperature etc. are factors that will affect the amounts of an element available for the different compartments of a tree growing at a specific site (Martin et al. 2006).

Martin et al. (2006) noted that the metal content of forest soil is highly variable over small distances, and that individual trees show highly different response because of varying small-scale (near-tree) conditions. Large between-tree variations in metal contents were ascribed to individual trees experiencing different micro-environments. The bioavailability of elements from the soil is dependent on a multitude of factors including soil pH, pE (redox conditions), water availability, mineral and organic content, fungi etc. (Kozlowski and Pallardy 1997, Martin et al. 2006). Garbe-Schönberg et al. (1997) also concluded that trees behave rather individualistically in their heavy metal uptake. In their study they found that levels of copper in birch and pine wood from two sites were similar even if the metal levels in the soil at the sites varied by a factor of 1000. The near-tree soil conditions thus have decisive influence on how varying concentrations of an element in the soil are reflected in the concentrations of the element in the wood of trees growing at the site.

Barks, and especially pine bark, has been used for monitoring of emissions of metal pollution to the atmosphere. In this kind of monitoring, the concentrations obtained from analyses of

bark samples from an area studied are generally evaluated by comparing them to results obtained for bark samples from background sites.

According to Pacheco and Freitas (2004) the use of lichen has been favoured above the use of tree bark in the monitoring of airborne contaminant, because of the expected effects related to root uptake of soil constituents on the latter. Based on results in the present thesis it can be recommended to analyse both bark and wood in environmental monitoring studies, preferably in connection with forest felling. This makes it possible to compare the elemental concentration in the stem bark to the concentration of this element in the wood on which the bark was developed. Ratios between the elemental concentrations in bark and wood, involve a normalisation for differences in bioavailability of the element from the soil at the sites where the trees have been growing.

If ratios between concentrations in the dry ashed materials are calculated, a normalisation is obtained also for the "general", and locally different, enrichment of inorganic elements from wood to bark. From Tables 10 and 11 it can be seen that:

- For samples from Harjavalta, the ash contents were, on average, 4 times higher in the stem bark than in the stem wood of both pine and spruce trees.
- For samples from Nagu, the ratios between ash contents of stem bark and stem wood were around 5 for pine, and around 7 for spruce trees.
- For samples from Ostrobothnia (mid-western Finland), the ratios were around 9 for both pine spruce.

Although there is a large enrichment of inorganic elements going from wood to bark, the concentrations of the elements in the ashes of respective material are mostly very similar. Considering analyses of dry ashed bark and wood for monitoring of atmospheric pollution, an upper limit seems to be set by calcium. The ratio between the concentration of Ca in bark ash and wood ash is around 2 for both pine and spruce. This ratio is generally the highest obtained for any element, when trees are from areas not exposed to any identified source of atmospheric pollution.

3.6.2. Elemental concentrations in stem wood and bark of pine, spruce and birch from unpolluted sites

The results from bulk analyses of stem wood and (whole) bark in **papers III-V,** and other earlier unpublished results are, summarised and evaluated in **paper VI**. Some of the main findings will be given in the following.

The compiled results from analyses of bark and wood from areas not affected by any identified source of environmental pollution are given in Table 12. The bark and wood samples analysed were from the same discs of trees but, in some cases, only the wood or the bark of a disc was analyzed. The samples were from a large number of different sites (islands, coastal and inland areas etc) and the relative standard deviations (RSDs) are large. The total of over 160 analyzed samples included in Table 12 give mean values that can serve as guideline values for concentrations to be expected in bark and wood of pine, spruce and birch.

Table 12. Results from PIXE analyses of stem bark and wood of the main tree species in Finland (Table 15, **paper VI**). Only elements present at quantifiable concentrations in all samples are included. The results are complemented with concentrations for Na, Mg and Al, obtained from Particle Induced Gamma Emission (PIGE) analyses (supporting paper 10) of pine (n=1) and spruce wood (n=7). All elemental concentrations are in mg/kg of dry material.

	Pine				Spruce				Birch			
Element	bark (n=21)		wood (n=37)		bark (n=25)		wood (n=36)		Bark (n=23)		Wood (n=21)	
	Mean	RSD	Mean	RSD	Mean	RSD	Mean	RSD	Mean	RSD	Mean	RSD
Ash [%]	2.03	58	0.304	18	3.85	40	0.422	46	1.76	38	0.328	32
P	482	89	76.1	59	853	46	80.7	93	295	85	145	51
S	834	69	92.0	40	1029	28	95.3	52	479	66	135	48
K	2147	86	625	35	5005	49	1121	85	2080	90	707	37
Ca	7938	63	752	26	19616	37	1016	38	6690	54	762	66
Mn	216	116	61.4	50	387	78	69.9	55	242	93	69.2	122
Fe	102	101	9.15	118	73.0	56	7.76	137	40.3	119	7.75	121
Cu	3.17	30	0.90	30	4.5	30	0.91	39	3.95	75	0.976	42
Zn	32.2	78	7.27	52	148	41	9.65	54	227	74	28.3	61
Rb	11.7	125	2.05	71	17.3	101	3.52	89	8.3	143	2.89	74
Sr	13.6	60	3.12	57	71.7	56	6.87	37	21.7	72	4.94	40
Na			*28.7*				*8.2*	*64.0*				
Mg			*86.0*				*108.0*	*36.0*				
Al			*3.1*				*6.7*	*40.0*				

Concentrations in ashes obtained from dry ashing of the materials presented in Table 12 are given in Table 13. The most striking in Table 13 is perhaps the very similar elemental concentrations in ashes of bark and wood, irrespective of the tree species. The ratios between concentrations in ashes of bark and wood in Table 13 are close to 1 for most elements, which means that the elements are enriched proportionally from wood to bark.

As also seen earlier, dividing the concentration of an element in the bark ash with that in the wood ash the highest ratio is generally obtained for calcium (2.1 for spruce in Table 13). According to Kozlowski and Pallardy (1997) surplus of Ca often accumulates as calcium oxalate crystals in cell vacuoles in leaves and woody tissue. High concentrations of calcium in bark have generally been attributed to the presence of calciumoxalate crystals (Fengel and Wegener 1984).

The lowest bark/wood ratio in Table 13 is generally seen for potassium. This could at least partly be related to poor binding capacity for this monovalent cation in the bark, and the fact that alkali metal ions form easily soluble salts.

Table 13 Elemental concentrations in ashes of the bark and wood samples presented in Table 12. All concentrations are given as **g/kg** of ash. The columns of values headed bark/wood give the ratios between the elemental concentrations in ashes of bark and wood.

	ashes of pine			ashes of spruce			ashes of birch		
Element	bark	wood	bark/wood	bark	wood	bark/wood	bark	wood	bark/wood
P	23.8	25.0	0.95	22.2	19.1	1.2	16.8	44.3	0.38
S	41.1	30.3	1.40	26.7	22.6	1.2	27.2	41.2	0.66
K	106	205	0.51	130	266	0.49	118	215	0.55
Ca	391	247	1.60	510	241	**2.1**	380	232	1.6
Mn	10.6	20.2	0.53	10.0	16.6	0.61	13.8	21.1	0.65
Fe	5.02	3.01	1.70	1.90	1.84	1.0	2.29	2.36	0.97
Cu	0.16	0.29	0.53	0.12	0.22	0.55	0.22	0.30	0.75
Zn	1.59	2.39	0.66	3.86	2.29	1.7	12.9	**8.62**	1.5
Rb	0.58	0.68	0.85	0.45	0.84	0.54	0.47	0.88	0.54
Sr	0.67	1.03	0.66	1.86	1.63	1.1	1.23	1.51	0.82
Na		9.44			1.94				
Mg		28.3			25.6				
Al		1.02			1.59				

As stated earlier, the differences between concentrations of an element in individual trees can be quite large. From the larger number of samples, from unpolluted sites, analysed for tables 12 and 13, some general conclusions can, however, be made:

- The elemental concentrations are very similar in the wood ashes of all tree species (Table 13). Similar concentrations were also seen for dry ashed eucalyptus wood in **paper IV.** The only clear exception is zinc in birch. Zinc is present in much higher concentrations both in wood and bark of this tree species. The special selectivity for uptake of zinc by the root system of birch is well illustrated by comparing concentrations in ashes of wood of different tree species as in **paper IV**.
- Inorganic elements can occur in up to around an order higher concentrations in the bark than in the wood of the stem (table 12). As established earlier (Tables 10 and 11 of section 3.6.1.), the general enrichment from wood to bark can be expressed by a ratio between the ash content of the stem bark and the stem wood, which is largely different between sites. The elemental compositions of the bark and the wood ashes in table 13 are, however, very similar. No strong selectivity for any element is thus seen in the formation of bark. The concentration of Ca in bark ash is about 2 times higher than the concentration of the element in the ash of the wood. This ratio of about 2 for calcium is in general the highest obtained for any element, when samples are from sites not exposed to any atmospheric pollution.
- The elemental concentrations in Table 13 represent a potential composition of elements in a total ash from combustion of the bio fuels. This composition reflects the uptake of the ions by trees, and the ash could thus favourably be used as fertiliser in, for example, forests. The bark has been said to amount to 10-20 % of a trunk (Fengel and Wegener 1984). As the ash contents are up to 9 times higher in bark than in wood, recycling of the bark ash could compensate for most of the inorganic element removed during logging. However, the possibility of high concentrations of heavy metals in bark is one aspect that should be considered. For the areas studied (Fig. 8 on page 27) this should be a problem only for bark from an area around the copper-nickel smelter at Harjavalta as well as from close to the zinc plant at Yxpihlaja, Kokkola (**paper VI**). Another consideration is the fact that the concentrations of calcium and potassium in the ashes of wood are close to identical, the Ca: K ratio is 1 (table 13). In ashes of bark, however, the Ca: K ratio is 4. Fertilising trees using ashes of tree bark could thus give a too high an input of Ca compared to the input of K. In pine needles, and a cone analysed, the concentrations of potassium were generally high, and higher than the concentrations of calcium (Table 11 in paper **VI**).

4. SUMMARY AND CONCLUDING REMARKS

Instrumentation for in-air PIXE (Particle Induce X-ray Emission spectrometry) analysis of thick solid samples has been developed at Åbo Akademi University. The samples were irradiated in air with 3 MeV protons from the MGC-20 cyclotron at the university. The particle beam was collimated to a diameter of 1 mm before extraction out of the vacuum system. A photomultiplier (PM) tube detected light emitted from the beam path between the beam exit window and the sample surface during proton irradiation. The integrated current from the PM tube during data acquisition was used for normalisation of the element specific yields, i.e. the peak areas in the accumulated spectrum. The set-up enabled quantitative multi-element analysis of solid wood materials, as well as the ashes of them. The quantification of the analyses was based on the use of biological certified reference materials (CRMs).

Data on concentrations of inorganic components in stem wood and bark of trees are relatively limited. Published data on the distribution of elements within these materials are often also contradictory. In this thesis results from analyses of stem bark and stem wood of Scots pine, Norway spruce and Silver birch are presented. The trees sampled were growing in south-western and mid-western Finland.

The set-up used in the PIXE analyses enables determination of elemental distributions on a millimetre-scale. Point scans on bark and wood samples were performed. Both bark and wood are heterogeneous materials. In bulk analysis, quite large amounts of these materials must therefore be properly homogenised to obtain elemental concentrations representative of the materials. Many (trace) elements are present at low concentration levels, which also puts demands on the sensitivity of the method. In this thesis, bulk analyses of stem bark and wood were performed by dry ashing the samples at 550 ˚C in prior to the PIXE analysis. The ashes were homogenised by shaking and prepared to target pellets for irradiation. The ash contents of, for example, wood samples were in the range 0.2-0.4 %, which meant that a large enrichment of the inorganic elements was obtained in the ashing procedure. By the direct analysis of the dry ashed materials, clearly lower detection limits were reached, which enabled quantitative determinations of some additional elements occurring at trace element level in the biological materials. The ash contents obtained from the dry ashing were also of importance in the evaluation of the results obtained from the analyses of bark.

The point scans performed revealed large variations of elemental concentrations in both stem bark and stem wood. When pine wood was scanned outwards, starting from the pith, the clearly highest concentrations of manganese, calcium and zinc were found in the first spot irradiated. The concentrations of these elements were from 2 (manganese) to over 3 (zinc) times higher in the pith than in the surrounding heartwood. For stem wood from the crown part of a pine, similar high concentrations were found in the first four spots (millimetres) of the scan, including the pith and the two following annual growth rings.

The lowest concentrations of zinc in a disc of pine stem wood were found in the innermost sapwood, i.e. the sapwood closest to the heartwood. Concentrations of zinc increased outwards in the sapwood towards the bark. An explanation for this finding could be a migration of zinc from sapwood being under transformation to heartwood. This kind of “recycling” of the element agrees with the role ascribed to zinc in woody plants as being a cofactor for RNA polymerase influencing protein synthesis.

The variations in elemental concentrations in heartwood were found to be small on the mm-scale. Point scans across sapwood of pine and spruce, on the other hand, showed more distinct variation in concentrations. Higher concentrations of, e.g., zinc, calcium and manganese were found in earlywood than in the denser latewood. Very high concentrations of iron and copper were also found in some local spots in earlywood increments. All together, the results obtained from point analyses of stem wood gave an overall picture of zinc as a very important trace element at the initial stages of the wood formation processes.

Barks, and especially pine bark, have been used for monitoring of emissions of metal pollution to the atmosphere. In published studies where pine bark is used, the concentrations in bark samples from monitored areas are usually compared to concentration obtained for bark samples from background sites.

The bulk analyses of bark (whole bark, i.e. all layers of the bark were sampled) in this thesis showed large variations for both elemental concentrations and ash contents of bark samples from the different areas sampled. The concentration of manganese was 14 times higher in pine stem bark from Ostrobothnia (mid-western Finland) than in pine stem bark from the island of Nagu. For pine samples from both areas it was, however, found that the ashes of the bark and the wood of tree stems had very similar elemental compositions. For samples from all non-polluted sites, the ratio between the concentration in the bark ash and the concentration in the wood ash had a value close to 1 for most elements. The highest ratio of around 2 was obtained for calcium, which actually was also the case for spruce and birch trees. Higher concentrations of plant available manganese in forest soil at Ostrobothnia was thus indicated by the above results for pine. The concentrations of zinc in ashes of birch stem bark were manifold higher than in the ashes of pine or spruce stem bark. The same was, however, the case also for the stem wood, and the bark ash/wood ash concentration ratio for zinc had a value close to 1 also for birch. This fact points out the extraordinary capability for uptake of zinc by this deciduous tree.

For pine trees sampled at 6 km from a copper-nickel smelter the ratios between bark ash and wood ash concentrations were high for Ni (ratio = 14), Fe (20), Cu (23) and Pb (28). For all other elements the ratio was less or equal to 2.3, the ratio obtained for calcium. The concentrations of copper were thus 23 times higher in ashes of the bark than in ashes of the wood of pine trees growing at this site. This confirms that basically all the copper in the pine bark originates from a direct atmospheric deposition, still at 6 km distance from the point source of emission.

One of the motives for using tree bark in air monitoring surveys is that, for example, Scots pine is available over large areas. The conditions affecting uptake and transport of the inorganic elements within a tree will, however, vary between sites. Based on results presented in this thesis a different approach for monitoring of inorganic atmospheric pollution, using bark, is suggested, where discs of pine wood are cut from the lower end of pine trees, preferable in connection with forest felling. The bark and the underlying stem wood of sectors of the discs are dry ashed and analysed separately (conveniently using PIXE applied as described in this thesis).

A ratio between the concentrations of an element in the ash of the bark and in the ash of the wood, involves normalisation for two main circumstances. Firstly, the bioavailability of element from the soil can be quite different at sites where trees are growing. Secondly, there

is a general enrichment of inorganic elements from wood to bark (most easily expressed by the ratio between the ash contents) which is locally different. Already a ratio >2 could reveal that the element appears as an atmospheric pollutant, i.e. deposition from the air is a greater source for accumulation of the element in the bark than is the soil-root-stemwood route. No comparison to selected background sites (samples) is thus needed if the above strategy is applied.

Knowledge of the elemental content of wood and other tree related materials has become of increasing interest in many areas during the last years. For example, input of heavy metal ions, with wood raw material, into pulping and paper processes has negative effects on bleaching chemicals. The increased use of wood based fuels also puts demand on the control of the heavy metal ion content in the fuel and the ashes generated in the combustion processes. In this thesis results from bulk analyses of a total of over 160 stem bark and wood samples are reported. The elements P, S, K, Ca, Mn, Fe, Cu, Zn, Rb and Sr were quantified in all samples. Complementary results obtained for Na, Mg and using Particle Induced Gamma Emission (PIGE) spectroscopy are also included. The presented concentration values may serve as guideline values for the elemental concentrations in bark and wood of logs of pine, spruce and birch.

As the PIXE analyses of stem bark and wood were performed on the ashes, obtained after dry ashing at 550 °C, the ash contents could be reported together with the elemental contents. The concentrations in the dry ashed materials represent elemental concentrations of total ashes obtainable from combustion of the biofuel materials. Knowledge of the chemical composition of the ashes is of great importance when considering the use of ashes as fertilisers, e.g., by recycling them back to the forest environment.

References

Aarnio P. A., Routti J. T. and Sandberg, J. V. (1988), MicroSAMPO – personal computer based advanced gamma spectrum analysis system, Radioanal. Nucl. Chem. vol. 124, pages 457-466.

Azcue J. and Mudrock A. (1997), Comparison of different washing, ashing and digestion methods for the analysis of trace elements in vegetation, Intern. J. Environ. Anal. Chem. Vol. 57, pages 151-162.

Berglund A., Brelid H., Rindby A. and Engström P. (1999), Spatial distribution of metal ions in spruce wood by synchrotron radiation microbeam X-ray fluorescence analysis, Holzforschung vol. 53, pages 474-480.

Bock R. (1979), A handbook of Decomposition methods in analytical chemistry, International Textbook Company, Edinburg, 444 pages.

Bull D. C. (2001), The chemistry of chromated copper arsenate II. Preservative-wood interactions, Wood Sci. Technol. vol. 34, pages 459-466.

Campbell J. L. and Cookson J. A. (1984), PIXE analysis of thick targets, Nucl. Instr. and Meth. vol. B3, pages 185-197.

Campbell J. L., Higuchi D., Maxwell J.A. and Teesdale W. J. (1993), Quantitative PIXE microanalysis of thick specimens, Nucl. Instr. and Meth. vol. B77, pages 95-109.

Clayton E. (1987), PIXE analysis of thick target biological samples in vacuum, Nucl. Instr. and Meth. vol. B22, pages 145-148.

Cookson J. A. (1988), Specimen damage by nuclear microbeams and its avoidance, Nucl. Instr. and Meth. vol. B30, pages 324-330.

Dahlbacka J. and Lindblom P. (1979), PIXE-analysis with 6 MeV H_2^+-ions, Physica Scripta vol. 20, pages 655-656.

Derome J. and Nieminen T. (1998), Metal and macronutrient flux in heavy-metal polluted Scots pine ecosystems in SW Finland, Environmental Pollution, vol. 103, pages 219-228.

Doyle B. L., Walsh D. S. and Lee S. R. (1991), External micro-ion-beam analysis (X-MIBA), Nucl. Instr. and Meth. vol. B54, pages 244-257.

Fengel D. and Wegener G. (1984), Wood: chemistry, ultrastucture and reactions, Walter de Gruyter & co, Berlin, 613 pages.

Folkmann F., Gaarde C., Huus T. and Kemp K. (1974), Proton Induced X-ray emission as a tool for trace element analysis, Nucl. Instr. and Meth. vol. 116, pages 487-499.

Garbe-Schönberg C.-D., Reimann C. and Pavlov V. A. (1997), Laser ablation ICP-MS analyses of tree-ring profiles in pine and birch from N Norway and NW Russia – a reliable record of the pollution history of the area?, Environmental Geochemistry vol. 32, pages 9-16.

Gloystein F. and Richter F-.W. (1987), A radiation thermometer for temperature control of thin samples during PIXE analysis, Nucl. Instr. and Meth. Vol. B 22, Pages 45-48.

Goclowski M., Jaskola M. and. Zemlo L. (1983), Comparison of different methods for eliminating the charge build-up on insulating samples in PIXE-analysis, Nucl. Instr. and Meth. vol. 204, pages 553-558.

Hansen L. D., Ryder J. F., Mangelson N. F., Hill M. W., Fausette K. J and Eatough D. J. (1980), Inaccuracies encountered in sulphur determination by particle Induced X-ray emission, Anal. Chem. Vol. 52, pages 821-824.

Hoenig M. (2001), preparation steps in environmental trace analysis – fact and traps, Talanta vol. 54, pages 1021-1038.

Hoenig M. (2003), Dry ashing, chapter 7 (pages 235-255) in: Sample Preparation for Trace Element Analysis (Eds. Mester Z. and Sturgen S.), Wilson and Wilsons Comprehensive Analytical chemistry, vol. XLI, Elsevier, Amsterdam.

Johansson S. A. E. and Campbell J. L. (1988), PIXE: A Novel Technique for Elemental Analysis, John Wiley & sons, New York, 347 pages.

Johansson S. A. E., Campbell J. L. and Malmqvist K. G. (Eds.) (1995), Particle Induced X-ray Emission Spectrometry (PIXE), Chemical Analyses, Vol. 133: A series of monographs on Analytical Chemistry and its Applications (J. D. Winefordrer, Series Ed.,), Wiley Interscience Publications, New York, 451 pages.

Johansson S. A. E. and Johansson T. B. (1976), Analytical application of particle Induced X-ray emission, Nucl. Instr. and Meth. vol. 137, pages 473-516.

Katsanos A. and Hadjiantoniou A. (1978), Sensitivity of the external beam PIXE elemental analysis method, Nucl. Instr. and Meth. vol. 149, pages 469-473.

Katsanos A., Xenoulis A., Hadjiantoniou A. and Fink R. W. (1976), An external beam technique for proton-induced X-ray emission analysis, Nucl Instr. and Meth. vol. 137, pages 119-124.

Kiikkilä O. (2003), Heavy-metal pollution and remediation of forest soil around the Harjavalta Cu-Ni smelter in SW Finland, Silva Fennica vol. 37, pages 399-415.

Knoll G. F. (1979), Radiation detection and measurement, John Wiley & sons, New York.

Koh S. Aoki T., Katayama Y. and Takada J. (1999), Losses of elements in plant samples under the dry ashing process, J. Radioanalytical Nucl. Chem. Vol. 239, pages 591-594.

Kozlowski T. T. and Pallardy S. G. (1997), Physiology of Wood Plants, 2nd edition, Academic Press, San Diego, 411 pages.

Kuczumov A., Larsson S. and Rindby A. (1996), Analysis of the distribution of inorganic components of wood by X-ray capillary microprobe, X-ray spectr. Vol. 25, pages 147-155.

Lill J.-O. (1999a), Charge Integration in external-beam PIXE, Nucl. Instr. and Meth. vol. B150, pages 114-117.

Lill J.-O. (1999b), Analys av fasta prov med jonstråle från en cyklotron, phil. lic. thesis, Åbo Akademi University, Turku, 100 pages.

Llorente M. J. F. and García J. E. C. (2005), Concentration of elements in woody and herbaceous biomass as a function of the dry ashing temperature, Fuel vol. 85, pages 1273-1279.

Lippo H., Poikolainen J. and Kubin E. (1995), The use of moss, lichen and pine bark in the nationwide monitoring of atmospheric heavy metal deposition in Finland, Water, Air and soil Pollut. Vol. 85, pages 2241-2246.

Lövestam G., Johansson E-M., Johansson S. and Pallon J. (1990a), Elemental micro patterns in tree rings – A feasibility study using scanning proton microprobe analysis, Ambio vol. 19, pages 87-93.

Lövestam N. E. G., Johansson E.-M., Johansson S.A.E. and Pallon J. (1990b), Scanning proton beam analysis applied to wood and bark samples, Nucl. Instr. and Meth. vol. B49, pages 490-494.

Mader P., Haber V. and Zelinka J. (1997), Classical dry ashing of biological and agricultural materials. Part I. Following the course of removal of organic matrix, Analusis vol. 25, pages 175-183.

Maenhaut W. (1987), Particle-induced X-ray emission spectrometry: an accurate technique in the analysis of biological environmental and geological samples, Analytica Chimica Acta vol. 195, pages 125-140.

Maenhaut W. (1988), Applications of ion beam analysis in biology and medicine, a review, Nucl. Instr. and Meth. Vol. B35, pages 388-403.

Maenhaut W. and Malmqvist K. G. (1992), Particle-Induced X-ray Emission Analysis, chapter 11 (pages 517-581) in: R. E. van Grieken and A. A. Markowicz (Eds.), Handbook of X-ray Spectrometry, Marcel Dekker, New York.

Malmqvist K. G. (1990), Quantitative PIXE analysis of biomedical material – sample preparation, irradiation and quality control, Nucl. Instr. and Meth. vol. B49, pages 183-190.

Mando P. A. (1994), Advantages and limitations of external beams in applications to arts & archaeology, geology and environmental problems, Nucl. Instr. and Meth. vol. B85, pages 815-823.

Martin R. R., Naftel S. J., Macfie S. M., Jones K. W., Feng H. and Trembley C. (2006), High variability of the metal content of tree growth rings as measured by synchrotron micro X-ray fluorescence spectrometry, X-ray spectr. Vol. 35, pages 57-62.

Martinsson B. G. (1987), External beam PIXE/PESA setup for characterisation of fine aerosols, Nucl. Instr. and Meth. vol. B22, pages 356-363.

Maxwell J. A., Campbell J. L. and Teesdale W. J. (1989), The Guelp PIXE software package, Nucl. Instr. and Meth. vol. B43, pages 218-230.

Meerts P. (2002), Mineral nutrient concentrations in sapwood and heartwood: a literature review, Ann. For. Sci. vol. 59, pages 713-722.

Nobiling R. (1986), High energy ion microprobes for surface analysis, Nucl. Instr. and Meth. vol. B14, pages 142-147.

Obernberger I. (1998), Decentralized biomass combustion: state of the art and future development, Biomass and Bioenergy, vol. 14, pages 33-56.

Pacheco A. M. G. and Freitas M. C. (2004), Are lower epiphytes really that better than higher plants for indicating airborn contaminants? An insight into the elemental contents of lichens thalli and tree bark by INAA, I. Journal of Radioanalytical and Nuclear Chemistry, vol. 259, pages 27-33.

Pallon J. and Malmqvist K. G. (1981), Evaluation of low temperature ashing of biological materials as a preconcentration method for PIXE analysis, Nucl. Instr. and Meth. vol. 181, pages 71-75.

Pihlman A. (2009), personal communication.

Poikolainen J. (1997), Sulphur and heavy metal concentrations in Scots pine bark in northern Finland and the Kola peninsula, Water, Air and Soil Pollut. Vol. 93, pages 395-408.

Pöykiö R., Perämäki P. and Niemelä M. (2005), The use of pine (*Pinus sylvestris* L.) bark as a bioindicator for environmental pollution monitoring along two industrial gradients in the Kemi-Tornio area, northern Finland, Intern. J. Environ. Anal. Chem., vol. 85, pages 127-139.

Raunemaa T., Hari P., Kukkonen J., Kulmala M. and Karhula M. (1987), Analysis of the bark of Scots pine as a method of studying environmental changes, Water air Soil Poll. Vol. 32, pages 445-453.

Roelandts I. and Gladney E. S. (1998), Consensus values for NIST biological and environmental Standard Reference Materials, Fresenius J. Anal. Chem. vol.360, pages 327-338.

Räisänen J. (1987), External-beam methods in biomedical work, Biol. Trace Elem. Res. Vol. 12, pages 55-64.

Räisänen J. (1989), Elemental analysis with external beam methods, Nucl. Instr. and Meth. vol. B40/41, pages 638-642.

Räisänen J. (1992), Experimental arrangements for non-vacuum Bio-PIXE, Intern. J. PIXE vol. 2, pages 339-350.

Schulz H., Popp P., Huhn G., Stärk H.-J. and Schűűrmann G. (1999), Biomonitoring of airborne inorganic and organic pollutants by means of pine tree barks. I. Temporal and spatial variations, Sci. Total Environ. vol. 232, pages 49-58.

Sjöström E. (1992), Wood chemisty: fundamentals and applications, 2nd edition, Academic Press, New York, 293 pages

Solin O., Kronman D., Lindblom P., Rosengård U. and Vuorinen K. (1988), Atomic near-infrared noble gas scintillations II. Application to particle beam intensity measurement, Nucl. Instr. and Meth. vol. A268, pages 209-211.

Szökefalvi-Nagy Z., Bakyinka Cs., Demeter I., Hollos-Nagy K. and Kovacs I. (1999), Specification of metal ions in proteins by combining PIXE and thin layer electrophoresis, Fresenius` J. Anal. Chem. Vol. 363, pages 469-473.

Teesdale W. J., Maxwell J. A., Perujo A., Campbell J. L., van der Zwan L. and Jackman T. E. (1988), Limits of detection and quantitation in PIXE analysis of thick targets, Nucl. Instr. and Meth. vol. B35, pages 57-66.

Themner K. (1991), Elemental losses from organic material caused by proton irradiation, Nucl. Instr. and Meth. vol. B54, pages 115-117.

Themner K., Spanne P. and Jones K. E. (1990), Mass loss during X-ray microanalyses, Nucl. Instr. and Meth. vol. B49, pages 52-59.

Tokareva E. N., Pranovich A. V., Fardim P., Daniel G. and Holmbom B. (2007), Analysis of wood tissue by time-of-flight secondary ion mass spectrometry, Holzforschung vol. 61, pages 647-655.

Wagner E. W. and Neelmeijer C. (1995), External proton beam analysis of layered objects, Fresenius' J. Anal. Chem. Vol. 353, pages 297-302.

Valkovic O., Jaksic M., Fazinic S., Valcovic V., Moschini G. and Menapace E. (1995), Quality control of PIXE and PIGE nuclear analytical techniques in geological and environmental applications, Nucl. Instr. and Meth. vol. B99, pages 372-375.

Watmough S. A. and Hutchinson T. C. (2003), Uptake of ^{207}Pb and ^{111}Cd through bark of mature sugar maple, white ash and pine: a field experiment, Environmental pollution vol. 121, pages 39-48.

Watmough S. A., Hutchinson T. C. and Evans R. D. (1999), The distribution of ^{67}Zn and ^{207}Pb applied to white spruce foliage at ambient concentrations under different pH regimes, Environmental and Experimental Botany, vol. 41, pages 83-92.

Watt F., Grime G. W. and Perry C. C. (1988), The damage of a 1 micron proton beam on a single pollen grain, Nucl. Instr. and Meth. vol. B30, pages 331-336.

Watt F., Thong P. S. P., Tan A. H. M. and Tang S. M. (1997), Nuclear microscopy of single cultured cells: beam damage studies, Nucl. Instr. and Meth. vol. B130, pages 188-191.

Werkelin J. (2008), Ash-forming elements and their chemical forms in woody biomass fuels, REPORT 08-06 of the Process Chemistry Centre, Faculty of technology, Åbo Akademi, (doctoral thesis)

Williams E. T. (1984), PIXE analysis with external beams: systems and applications, Nucl. Instr. and Meth. vol. B3, pages 211.

Väisänen A., Laatikainen P., Ilander A., Renvall S. (2008), Determination of mineral and trace elements concentrations in pine needles by ICP-OES: evaluation of different sample pre-treatment methods, Inter. J. Environ. Anal. Chem. Vol. 88, pages 1005-1016.

Zeng X., Wu X., Shao Q., Tang J. and Yang F. (1990), Radiation damage in PIXE analyses of museum paper-like objects, Nucl. Instr. and Meth. vol. B47, pages 143-147.

Ziegler J. F., Manual for: TRIM, The Transport of Ions in Matter (version 95.xx), IBM-research, Yorktown, NY, USA.

Ziegler J. F., Biersack J. P. and Littmark U. (1985), The stopping and range of ions in solids, Pergamon Press, New York.

APPENDIX 1

Concentrations in Certified biological (plant) Reference Materials. Certified values are completed with concensus values, and concentrations in ashes are calculated using the ash-% obtained from dry-ashing at 550 ˚C. All elemental concentrations are in mg/kg of dry material.

	Tomato Leaves				Energy grass				Beech Leaves				Energy Forest				Pine Needles				Wood Fuel			
	In biological		in ashes		In biological		in ashes		In biological		in ashes		In biological		in ashes		In biological		in ashes		In biological		in ashes	
	conc.	±	conc.	±	conc.	±	conc.	±	conc.	±	conc.	±	conc.	±	conc.	±	conc.	±	conc.	±	conc.	±	conc.	±
ash-%	19.4				6.26				6.10				1.57				2.52				1.233			
Ca	30000	300	154000	2000	2100	180	33500	2900	5300	50	86900	800	4400	180	279000	11000	4100	200	163000	8000	3500	220	284000	18000
K	44600	300	229000	2000	3800	210	60700	3400	9940	200	163000	3000	2000	350	127000	22000	3700	200	146000	8000	900	17	73000	1400
P	3400	200	18000	1000	1090	90	17400	1400	1550	40	25400	700	500	100	32000	6000	1200	200	48000	8000	210	28	17000	2300
Mg	6600	400	34000	2000	880	74	14100	1200	878	17	14400	300	340	36	22000	2300	1180	120	46800	4800	300	18	24300	1500
Si	10500	700	54100	3600	21000	2400	335000	38000					120	31	7600	1970	1290	90	51200	3600	230	37	18700	3000
Al	1130	260	5820	1340	1800	170	28700	2700	435	4	7130	70	20	15	1300	950	545	30	21600	1200	260	32	21100	2600
Mn	238	7	1230	40	160	16	2600	300	1300		21311	0	60	11	3800	700	675	15	26800	600	210	38	17000	3100
Fe	690	25	3550	130	1060	63	16900	1010	550		9016		26	7.2	1650	460	200	10	7900	400	70	17	5700	1400
Na					300	150	4790	2400					29	4.3	1840	270	36	16	1400	630	40	12	3200	970
Zn	62	6	320	30	42	4.2	670	70	69		1131	0	75	5.0	4800	320	65	8	2600	300	38	8.5	3100	690
Rb	16.5	0.1	85.0	0.5													11.7	0.1	464	4				
Sr	44.9	0.3	231	2													4.8	0.2	190	8				
Pb	6.3	0.3	32	2	2.1	0.43	34	7	16.3		267	0	0.14	0.01	8.9	0.9	10.8	0.5	429	20	0.68	0.025	55	2.0
Cu	11	1	57	5	6.8	0.46	109	7	12.0		197		4.00	0.38	254	24	3.0	0.3	120	10	2.2	0.3	180	24
Ni	1.20	0.16	6.19	0.82													2.7	0.6	107	24				
Cr	4.5	0.5	23	3	3.4	0.68	54	11	8.0	0.6	130	10					2.6	0.2	100	10	0.8	0.3	65	24
Cd	2.7	0.3	13.9	1.5	0.09	0.023	1.4	0.4	0.34		5.6		1.8	0.14	114	9	0.21	0.05	8.3	2.0	0.27	0.028	22	2.3
Cl	10500	700	54100	3600	580	44	9300	700	1490	60	24400	900	100	61	6400	3900	296	58	11700	2300	100	36	8110	2920
Br	22	2	113	10													7.5	1.3	298	52.0				
As	0.27	0.05	1.4	0.3	0.40	0.12	6.4	1.9									0.21	0.04	8.3	1.6	0.80	0.24	65	19
Ti					130	24	2080	380													2.4	0.44	195	36
S-%	0.61	0.04	3.1	0.21	0.132	0.010	2.11	0.15	0.269	0.004	4.41	0.07	0.026	0.0053	1.7	0.3	0.1250	0.0130	4.96	0.515873	0.018	0.004	1.5	0.32
C-%					46	1							49.0	0.96			50.1	0.5			51	1.1		
H-%					5.7	0.14							6.05	0.043			6.49	0.34			6.04	0.082		
N	4.93	0.03			1.04	0.068			2.629	0.025			0.37	0.059			1.10	0.12			0.17	0.050		
Concensus values by Roelandts and Gladney (1998) for: Mg(n=37), S(13), N(6), Br(19), Cd(51), Si(7), Al (n=17), Ni (n=10), Cl (n=6)					Information values only for C, H, Na and Ti				Information values only for: Cd, Cu, Fe, Mn, Pb and Zn				Information values only for: C, H, Cl, Al, Si and Pb				Concensus values by Roelandts and Gladey (1998) for: N (n=8), Mg(48), Si(10), Cl(9) Ni(30), Br(22), Cd(30), Zn(54), Na(21), S(20), C(8), H(8)				Information values only for: C, H, N, Cl, Si and Ti			